Encyclopedia of Environmental Control Technology

VOLUME 2

Air Pollution Control

Paul N. Cheremisinoff, Editor

Encyclopedia of Environmental Control Technology

VOLUME 2

Air Pollution Control

Library of Congress Cataloging-in-Publication Data
Air pollution control.
(Encyclopedia of environmental control technology; v. 2)
Includes index.
1. Air—Pollution. 2. Air—Pollution—Measurement. 3. Air quality management. I. Cheremisinoff, Paul N. II. Series.
TD191.5.E5 vol. 2 [TD883] 628.5 s [628.5'3] 88-24280
ISBN 0-87201-245-X
ISBN 0-87201-238-7 (series)

CHAPTER 5

SIMULATING SHORT-TERM, SHORT-RANGE AIR QUALITY DISPERSION PHENOMENA

Paolo Zannetti

AeroVironment Inc.
Monrovia, California, USA

CONTENTS

INTRODUCTION AND OVERVIEW

Atmospheric dispersion phenomena occur mostly in the lower part of the atmosphere, called the Planetary Boundary Layer (PBL). This region extends from the earth's surface to

the top (z_i) of the PBL, where z_i varies from about 100 m to 2 km, with typical values in the range of 500–1,000 m. The PBL is "the region in which the atmosphere experiences surface effects through vertical exchanges of momentum, heat, and moisture" [1], and the top of the PBL, z_i, is "the lowest layer in the atmosphere at which the ground surface no longer influences the dependent (meteorological) variables through the turbulent transfer of mass" [2].

Above the PBL, in the "free" atmosphere where atmospheric turbulence is virtually nonexistent, dispersion still occurs, but at much lower rates. For this reason, and because human activities occur almost totally within the PBL, atmospheric disperison studies mostly focus on the PBL.

Transport Scales

Air quality dispersion phenomena can be characterized in several ways. A fundamental distinction is based upon the transport scale:

1. Near-field phenomena—less than 1 km from the source. This is the region where plume buoyancy and local effects, such as the downwash of a plume caused by a building, are important.
2. Short-range transport—up to 10 km from the source. This is the area of maximum ground-level impact for the primary pollutants (i.e., those pollutants that are directly emitted from the sources).
3. Intermediate transport—10 to 100 km from the source. In this region, impacts, including ground deposition, of secondary pollutants formed in the atmosphere from chemical and photochemical reactions of primary pollutants become noticeable.
4. Long-range (or regional, or interstate) transport—at distances greater than 100 km. Here large-scale meteorological patterns, chemical transformations, and deposition rates play the most important role.
5. Global transport, such as the stratospheric transport of radioactive material and volcanic emissions, and the global atmospheric buildup of carbon dioxide.

This chapter focuses on near-field and short-range phenomena, in which atmospheric chemistry and ground deposition generally play a negligible role, and atmospheric turbulence is the key factor in assessing the impacts of instantaneous or continuous emissions.

Over the last 10–15 years, the media and the scientific community have given increasing interest and attention to intermediate, long-range, and global processes, due to awareness of problems such as acidic deposition, carbon dioxide accumulation, stratospheric ozone depletion, etc. Recent accidents, however, such as the lethal one in Bhopal, India, have renewed the interest in short-range simulation of short-term exposures, especially in connection with accidental releases of toxic heavy gases, with the aims of better understanding the physics of the problem and of providing short-term emergency response systems, based on real-time forecasting of the dispersion of an accidental release.

Simulation Modeling

Modeling is the key tool for any quantitative understanding of atmospheric dispersion. Three types of models are commonly used:

1. Analytical models } Mathematical models
2. Numerical models }
3. Physical models

Analytical models are based on analytical explicit solutions of diffusion equations. These solutions can be found only under simple assumptions, such as homogeneous and stationary conditions. Analytical models do not necessarily require a computer, but most of them have been implemented in software to facilitate application.

Numerical models are based on numerical approximations (such as by finite-difference methods) of partial differential equations representing atmospheric dispersion phenomena. They can handle, at least theoretically, nonstationary, nonhomogeneous conditions and complex configurations of the spatial domain, such as rough terrain. They can be applied only through computer software.

Physical models are small-scale representations of atmospheric dispersion. They include wind tunnels, water tanks, and smog chambers. They can be very useful in providing semiquantitative results under complex dispersion scenarios that would otherwise be difficult to evaluate. Although this survey does not discuss physical models, further information can be found in [3–6].

All three modeling approaches are *deterministic*, i.e., they are based on the establishment of a cause-effect relationship between the emission of atmospheric pollutants and ambient air quality concentrations. Only deterministic models can provide quantitative answers to the "what if" questions, such as "what if certain emissions are reduced by 30%?" or "what if new emissions are added to the present emission scenario?" Thus, deterministic dispersion models are indispensable in evaluating alternative emission scenarios for urban and industrial planning.

In other cases, however, a second category of models, the *statistical* models, is useful.

Statistical Models

Statistical models are based on statistical analysis of measurement data, mostly time series of meteorological and air quality data. These statistical methods can often identify trends, similarities, and correlations that allow important semiquantitative conclusions to be drawn on specific air quality issues.

There are several reasons for using, in some applications, statistical rather than deterministic models. In particular:

- Statistical models are quite useful in real-time, short-term forecasting, since they can, to some degree, take into account unknown variations in input data (e.g., emission rates).
- Statistical (or mixed deterministic-statistical) predictors allow *all* available data (emission, meteorology, *and concentrations*) to be used in forecasting computations.
- Often, the information available from measured concentration data (e.g., trends) at times close to the forecasting time is more relevant than that obtained from deterministic simulations.
- Statistical predictors often have adaptive capabilities that make them useful even in regions, and during periods, different from those in which they have been calibrated.

In spite of these advantages, however, purely statistical models lack physical, deterministic relations and, therefore, cannot be used for regulatory application and precise evaluations of source-receptor contributions. Further information on statistical models can be found in Georgopulos and Seinfeld [7] for the statistical distribution of concentration measurements, Zannetti [8] for time-series analysis, and Simpson and Layton [9] and Tiao et al. [10], for application of the Box-Jenkins theory.

Statistical models will not be further discussed in this chapter. However, one type of recently developed statistical model, receptor modeling, deserves some additional discussion.

Receptor Models

While dispersion models compute the contribution of a source to a receptor as the product of the emission rate by a dispersion factor, receptor models start with the ambient aerosol concentrations observed at a receptor and seek to apportion the observed concentrations to several source types (e.g., industrial, transportation, soil, etc.), based on the chemical composition (i.e., the chemical fractions) of the source and receptor materials. This source apportionment can be performed using simple techniques such as the chemical mass balance (CMB), or more complex ones such as factor analysis. Receptor models have been reviewed by Cooper and Watson [11], Kleinman et al. [12], Gordon [13], Watson [14] and Henry et al. [15]. While they are an interesting alternative approach to dispersion modeling, they seem to be strongly affected by input data errors; however, their joint application with deterministic models (mixed approach) seems quite promising. This possible joint application is schematically illustrated in Figure 1.

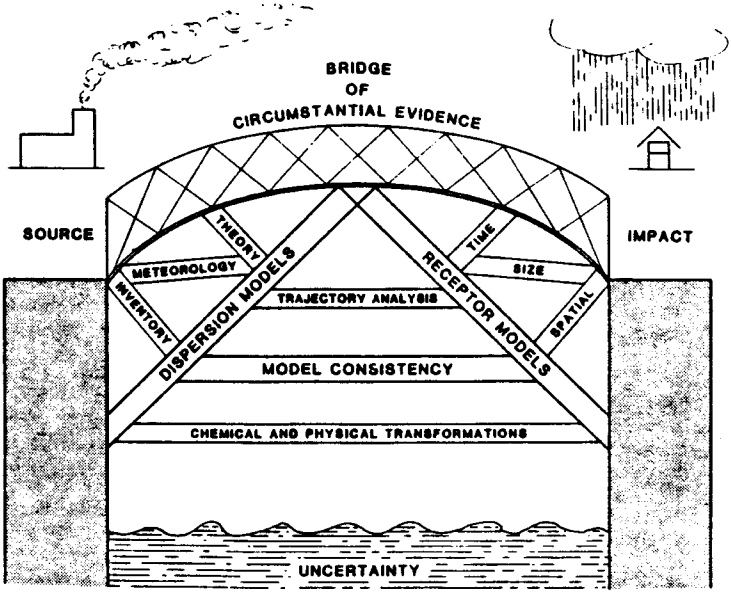

Figure 1. Schematic illustration of the need to use many different independent approaches to establish a strong bridge of circumstantial evidence quantitatively linking a source to its impact [15a]. Reprinted with permission from *Pollution Atmospherique.*

A Guide to This Chapter

As previously mentioned, this chapter deals with deterministic mathematical techniques for the simulation of short-term, short-range air quality dispersion phenomena. In the following sections, we describe the different components, or "modules," that can be used in this simulation. First, meteorological models, which provide the input to dispersion models, are

discussed. Plume rise phenomena are presented in "Plume Rise Formulations," and the next three sections analyze the major categories of dispersion models: the Eulerian models, in which the computational domain is divided into grid cells; the Gaussian models, which are based on the explicit Gaussian dispersion formula; and the Lagrangian models, in which the reference system moves with the average wind speed and direction. The final section discusses a few special applications of dispersion models.

METEOROLOGICAL MODELS

Meteorological models have been developed for two major goals:

1. Understanding local, regional, or global meteorological phenomena.
2. Providing the meteorological input of wind and atmospheric turbulence required by air pollution dispersion models.

In this chapter, we will focus our attention on the second group of meteorological models; i.e., on those techniques used to "preprocess" available meteorological information in order to prepare the proper input to air quality dispersion models.

A book by Pielke [2] provides a thorough review of mesoscale (i.e., from a few kilometers to several hundred kilometers) meteorological modeling techniques. This book also presents, in its Appendix B, a summary of the main organizations active in prognostic numerical mesoscale modeling and a list of existing mesoscale models, with their major characteristics.

Meteorological models can be:

1. Analytical models, in which exact analytical solutions are obtained.
2. Numerical models, in which approximate numerical solutions are found using mainly numerical integration techniques.

In this chapter, we will treat only numerical models, which are currently the most powerful and promising tools for both meteorological and air quality simulation studies.

Numerical models can be divided into two groups:

1. Diagnostic models, i.e., those with no time-tendency terms.
2. Prognostic models, i.e., those with full time-dependent equations.

These two groups are discussed further below. Clearly, the complexity of the meteorological model to be used depends upon the complexity of the diffusion model. In fact, simple diffusion models, such as the simplest Gaussian methods, cannot make full use of three-dimensional meteorological input, but these data can be used effectively by more advanced dispersion techniques.

Diagnostic Models

Diagnostic models are based on objective analysis of available meteorological data. Their output is usually a three-dimensional field of meteorological parameters, derived by interpolation and extrapolation of meteorological measurements. These models are diagnostic because they cannot be used to forecast the meteorological evolution, but simply provide a best estimate of a steady-state condition.

Diagnostic models have been used widely to evaluate mass-consistent flow fields in complex terrain (e.g., [16–18]). A mass-consistent method based on principal component analysis, developed by Ludwig and Bird [19], seems quite cost-effective. Diagnostic models based on mass-consistent flow calculations give satisfactory results [2] when:

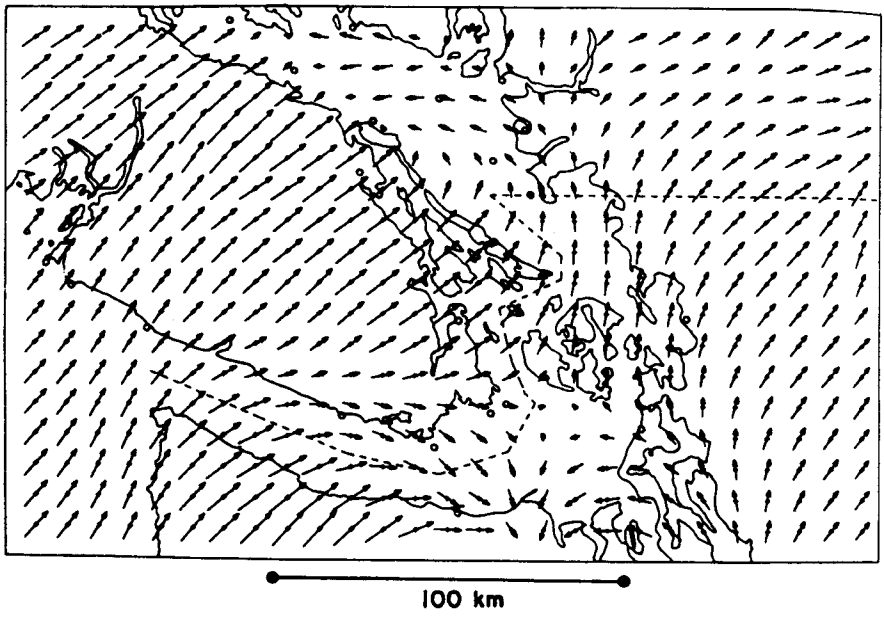

Figure 2. Winds simulated by a diagnostic model over the region around the southern end of Vancouver Island, British Columbia. Wind arrows are centered in each grid point and one grid distance represents 10 m s^{-1} [19a]. Reprinted with permission from the American Meteorological Society.

- The terrain is the dominant forcing term
- A strong elevated inversion is present below the highest terrain height
- Sufficient meteorological input measurements are available

Figure 2 is an example of diagnostic model output.

Diagnostic models rely on computational techniques (also called objective analysis methods), which are applied for, among other things, performing:

- Spatial interpolation/extrapolation of wind measurements
- Spatial interpolation/extrapolation of stability measurements
- Divergence-free corrections to the wind field
- Empirical computations for taking into account terrain effects (e.g., sea and valley breezes)

Diagnostic methods provide, as a minimum, a three-dimensional wind field in basic agreement with wind observations that can be used for dispersion calculations.

Prognostic Models

Prognostic meteorological models forecast the time evolution of the atmospheric system through the space-time integration of the equations for the conservation of mass, heat, motion, and water. Pielke [2] discusses these equations. Three additional equations (the ideal gas law, and definitions of potential and virtual temperature) are also used. This total set of equations consists of 11 simultaneous nonlinear partial differential equations in 11 dependent

variables (density, potential temperature, temperature, virtual temperature, pressure, three wind components, and density of water in three forms). The independent variables are the time t and the spatial coordinates x, y, and z.

To be complete, the above set of equations should include conservation relations for other atmospheric chemical species besides water; e.g., gaseous material, such as sulfur dioxide, and aerosols, such as sulfates and nitrates. However, the simultaneous solution of both (a) meteorological equations and (b) pollutant transport, diffusion, chemistry and deposition equations, represents a formidable problem. It is, therefore, commonly assumed that the concentration of primary and secondary atmospheric pollutants do not affect the meteorology. Consequently, prognostic meteorological models can be applied generally and run independently of the dispersion models (i.e., as preprocessors).

Prognostic meteorological modeling aims at finding the solution of the aforementioned 11 equations, or a subset of them. Modifications and simplifications of these basic equations are, however, required to permit their solution.

Several prognostic meteorological models have been developed. Unfortunately, most of them are complex research tools whose correct use generally requires the active involvement of the developers of these models. A comprehensive list of current mesoscale numerical models and their characteristics is presented in Appendix B of Pielke [2]. The development of two advanced meteorological models has been particularly important: the three-dimensional URBMET vorticity-mode model developed by Bornstein [20], and the primitive equation-mode model developed by Pielke et al. [21]. The former has the distinguished feature of introducing the stream function and three-dimensional vorticity vector in the equation of conservation of motion.

Especially when data measurements are scarce, prognostic models are the best tool to provide the appropriate meteorological input to advanced dispersion models. However, much research is still needed for the improvement of these models in order to provide:

1. An evaluation of small-scale sub-grid turbulence parameters.
2. Real-time predictive capabilities using meteorological measurements to adjust the forecasts.
3. The evaluation of the special meteorological input required by Lagrangian dispersion models. (See "Lagrangian Dispersion Models.")

PLUME RISE FORMULATIONS

In most cases, pollutants injected into ambient air possess a higher temperature than the surrounding air. Most industrial pollutants, moreover, are emitted from smokestacks or chimneys, and therefore possess an initial vertical momentum. Both factors (thermal buoyancy and vertical momentum) contribute to plume rise. This process ends when the plume's initial buoyancy is lost by mixing with the ambient air.

The physical consequence of the above phenomenon is generally quantified by a single parameter, the plume rise Δh, defined as the *vertical displacement of the plume* in this initial phase. Several studies have provided semi-empirical formulas for evaluating Δh (e.g., [22]); others have provided more complex and complete description of the several physical interactions between the plume and the ambient air (e.g., [23]).

Semi-Empirical Δh Formulations

A review of the available semi-empirical formulations for computing Δh (and its variation with the downwind distance from the source) is presented by Strom (in Stern [24]) and Hanna et al. [25]. Most equations for Δh have the following form:

$$\Delta h(x) = \text{const}\ Q_h^a\ x^b\ u^c \tag{1}$$

where const, a, b, c = constants
x = downwind distance
u = wind speed

Q_h is the heat emission rate of the source, given by:

$$Q_h = Q_m\ c_p\ (T_s - T_a) \tag{2}$$

where c_p = specific heat at constant pressure
T_s = gas exit temperature
T_a = ambient temperature

Q_m is the total mass emission rate, given by:

$$Q_m = \rho_s\ \pi\ r_s^2\ v_s \tag{3}$$

where ρ_s = mass density of the total emission
r_s = exit radius
v_s = exit speed.

Among the various schemes, the Briggs [22] method is the most widely applied, especially for U.S. regulatory applications. The method defines the buoyancy flux parameter:

$$F_b = g\ v_s r_s^2 (T_s - T_a)/T_s \tag{4}$$

where g = gravity acceleration constant

and the critical downwind distance x*:

$$x^* = 2.16\ F_b^{2/5}\ z_s^{3/5}, \text{ for } z_s < 305 \text{ m} \tag{5}$$

$$x^* = 67\ F_b^{2/5}, \text{ for } z_s \geq 305 \text{ m} \tag{6}$$

where z_s = source height

For $x \leq x^*$, the formula:

$$\Delta h(x) = \text{const}\ F_b^{1/3} u^{-1} x^{2/3} \tag{7}$$

is used (with const between 1.6 and 1.8), while for $x > x^*$ the formula is:

$$\Delta h(x) = 1.6\ F_b^{1/3} u^{-1} x^{*2/3} \left[\frac{2}{5} + \frac{16}{25}\frac{x}{x^*} + \frac{11}{5}\left(\frac{x}{x^*}\right)^2\right]\left(1 + \frac{4}{5}\frac{x}{x^*}\right)^{-2} \tag{8}$$

Equations 7 and 8 are used for buoyant plumes, i.e., when $T_s > T_a$. Cold plumes (jets) can be treated by similar equations. For example, according to Briggs [26], the plume rise of a jet is:

$$\Delta h(x) = 2.3\ F_m^{1/3} u^{-2/3} x^{1/3} \tag{9}$$

where the momentum flux parameter is:

$$F_m = v_s^2 r_s^2\ \rho_s/\rho \simeq v_s^2 r_s^2 \tag{10}$$

where ρ = density of the air.

In calm conditions ($u \simeq 0$), the above formulas cannot be used. In these situations, Briggs [22] suggests the following equations for the final plume rise:

$$\Delta h = 5.0\ F^{1/4} s^{-3/8} \text{ for buoyant plumes} \tag{11}$$

$$\Delta h = 4.0\ F_m^{1/4} s^{-1/4} \text{ for jets} \tag{12}$$

where s is the stability parameter:

$$s = \frac{g}{\theta} \frac{\partial \theta}{\partial z} \tag{13}$$

and θ is the potential temperature.

Turner [27] gives a generalized routine that calculates both plume rise and partial penetration of the plume into the layer above the mixing height. This routine assumes that meteorological data (temperature and wind speed) are available by layers and that the mixing height h* and the potential temperature gradient $\partial\theta/\partial z$ above the mixing height are known. The method is based on the following steps:

1. Calculation of f, the stack tip downwash correction factor, with the method of Bjorklund and Bowers [28]. The parameter f is computed by first evaluating the Froude number F_r:

$$F_r = \frac{v_s^2}{2\ g r_s\ (T_s - T_a)/T_a} \tag{14}$$

Then:

if $F_r < 3$, $f = 1$

if $F_r \geq 3$ and $v_s \leq u$, $\Delta h = 0$

if $F_r \geq 3$ and $v_s > 1.5\ u$, $f = 1$

* In neutral and unstable conditions, it is $h = z_i$. In stable conditions, where z_i is the thickness of the ground-based inversion layer, mechanical turbulence creates a mixing layer from $z = 0$ to $z = h$, where $h < z_i$.

otherwise:

$$f = 3(v_s - u)/v_s \tag{15}$$

2. Calculation of the plume rise Δh by layers. If the plume rise exceeds the top of a layer, computations are repeated for the next layer above using the residual plume buoyancy. Computations are made using formulas similar to those by Briggs described before.
3. Calculation of the actual final plume rise $\Delta h'$:

$$\Delta h' = f\Delta h \tag{16}$$

to incorporate stack tip downwash effects when $f < 1$.

4. Incorporation of plume penetration of the mixing height by decreasing the mass emission rate Q of the pollutant and further adjusting the plume rise. More specifically, the bottom and the top of the plume are computed as:

$$b_p = z_s + 0.5\ \Delta h' \tag{17}$$

$$t_p = z_s + 1.5\ \Delta h' \tag{18}$$

respectively. If $b_p > h$, the pollutant emission rate is set equal to 0, since the plume is assumed to contribute nothing inside the mixing layer and to remain trapped in the stable layer above it. Otherwise, if $t_p > h$, the plume rise is further corrected as:

$$\Delta h'' = \frac{h - b_p}{2} - z_s \tag{19}$$

and the pollutant emission rate is set equal to $f'Q$, where:

$$f' = \frac{h - b_p}{\Delta h'} \tag{20}$$

in order to eliminate the contribution of the fraction $(1 - f')$ of the plume that has perforated the mixing height h.

Advanced Plume Rise Models

The formulations presented in the previous section have shown, on several occasions, a great degree of uncertainty. Additional methods have been proposed that provide, at least in theory, a better physical representation of the two basic phenomena related to the plume rise:

- The vertical increase of the plume centerline
- The entrainment of ambient air into the plume and its consequent horizontal and vertical spreading

Among the second group of formulations is the integral plume rise model of Schatzmann [29], which allows a numerical solution of the equations of the conservation of mass, momentum, concentration, and thermal energy. This method seems particularly effective since

it does not use the common Boussinesq approximation and, therefore, allows the treatment of jet flow with density greatly different from that of ambient air.

An even more complex approach, a differential entrainment model, has been proposed by Golay [23]. It can simulate bent-over plumes in complicated vertical atmospheric structures by numerically integrating the conservation equations of mass, momentum, heat, water vapor, liquid water, and the two equations for the turbulent kinetic energy and eddy viscosity in the form presented by Stuhmiller [30]. The major limitation of the Golay approach is the detailed meteorological input required, i.e., the vertical profiles of wind speed, virtual potential temperature, relative humidity, turbulence kinetic energy, and turbulent viscosity.

Glendening et al. [31] have proposed a simpler approach that numerically integrates the conservation equations, using several simplifying assumptions (e.g., the plume is axisymmetric and its three-dimensionality is ignored).

Special plume rise formulations are available for special cases, such as:

- Plume rise from multiple sources [22, 32]
- Partial penetration by the plume of an elevated inversion layer [33]
- Plumes from stacks with scrubbers, whose significant moisture content seems to require ad-hoc techniques [34]

Again, as for the meteorological models, the complexity of the plume rise formulation must be consistent with the complexity of the dispersion model to be used.

EULERIAN DISPERSION MODELS

Air pollution diffusion can be simulated by several techniques, primarily in two categories:

1. Eulerian models
2. Lagrangian models

The basic difference between the Eulerian and Lagrangian view is illustrated in Figure 3, in which the Eulerian reference system is fixed (e.g., with respect to the earth) while the Lagrangian reference system follows the average atmospheric motion. Several authors, and in particular Lamb (from [35]), have investigated the two approaches and their interrelationships in detail, as summarized in Figure 4. This section presents the fundamentals of the Eulerian approach and the major Eulerian modeling techniques for atmospheric diffusion. Lagrangian methods are discussed later.

The Eulerian Approach

The Eulerian approach is based [35] on the conservation of mass of a single pollutant species of concentration c(x, y, z, t).

$$\frac{\partial c}{\partial t} = -\mathbf{V} \cdot \nabla c + D\nabla^2 c + S \tag{21}$$

where $\mathbf{V}(x,y,z,t)$ = wind vector
D = molecular diffusivity (about $1.5\ 10^{-5}$ m^2/s for air)
∇ = gradient operator
$\nabla^2 = \partial^2/\partial x^2 + \partial^2/\partial y^2 + \partial^2/\partial z^2$ = Laplacian operator
$S(x,y,z,t)$ = pollutant source term

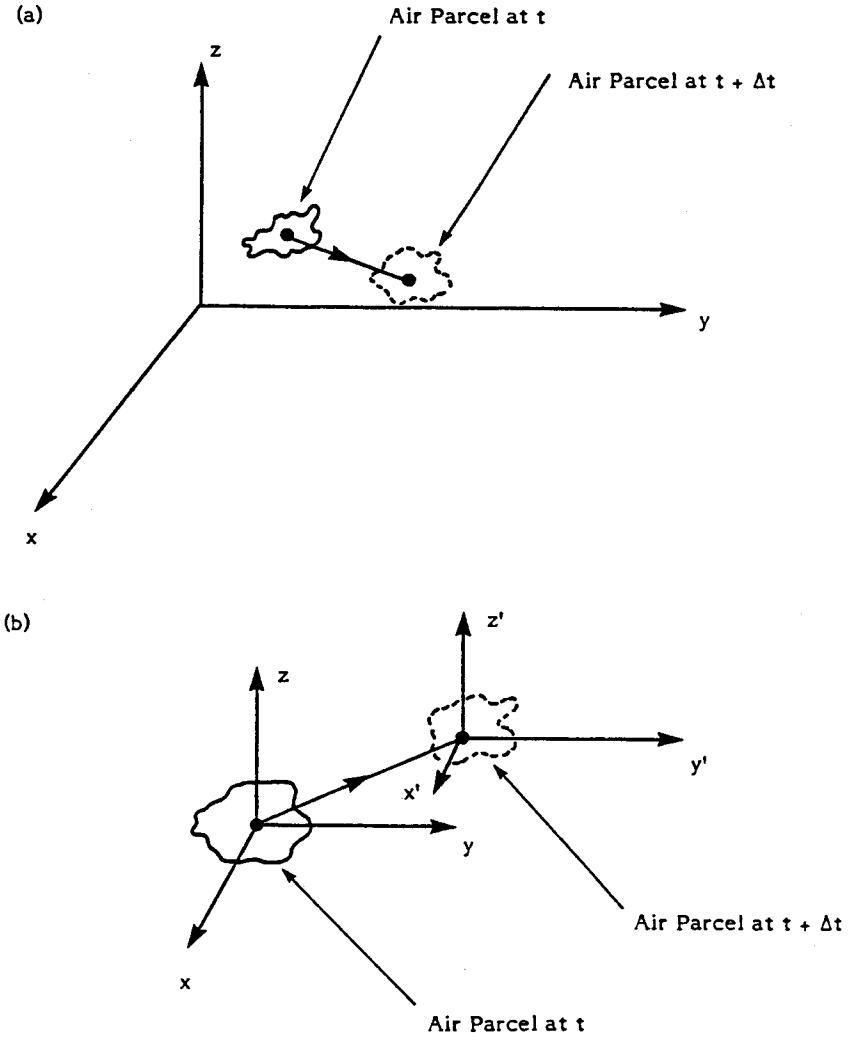

Figure 3. Eulerian (a) and Lagrangian (b) reference systems for atmospheric motion.

The velocity is assumed to be representable as the sum of "average" and "fluctuating" components:

$$\mathbf{V} = \bar{\mathbf{u}} + \mathbf{u}' \tag{22}$$

where $\bar{\mathbf{u}}$ represents the portion of the flow that is resolvable using meteorological models (i.e., $\bar{\mathbf{u}}$ is provided by one of the meteorological models discussed earlier), and $\mathbf{u}'$ is the

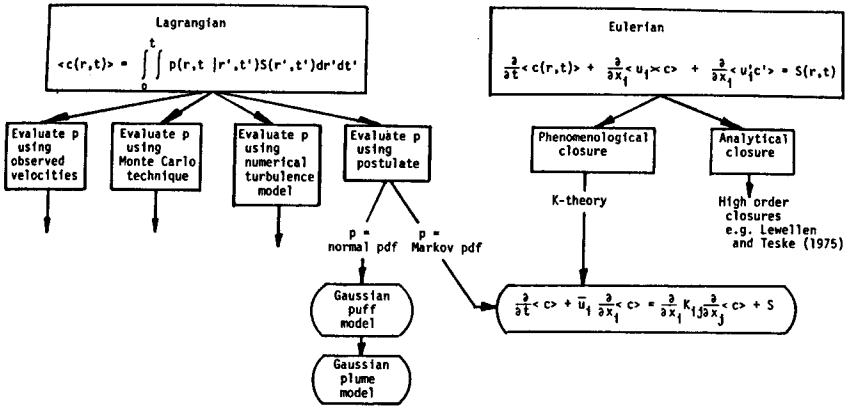

Figure 4. Schematic illustration of relationships among the Eulerian and Lagrangian models of turbulent diffusion. (From Lamb in [35]. Reprinted with permission from Elsevier Science Publishers B. V.)

remaining unresolvable component, a stochastic variable, since there exists an infinite family of functions $\mathbf{u}'$ that satisfy the equation of motion. A second assumption is that:

$$c = \langle c \rangle + c' \tag{23}$$

where $\langle\ \rangle$ denotes the ensemble (theoretical) mean, i.e., the average, at a certain point and time, of all possible concentrations generated by each member of the infinite family of functions $\mathbf{u}'$. Then, substituting Equations 22 and 23 in 21 and taking the ensemble average, we obtain:

$$\frac{\partial \langle c \rangle}{\partial t} = -\bar{\mathbf{u}} \cdot \nabla \langle c \rangle - \nabla \cdot \langle c'u' \rangle + D\nabla^2 \langle c \rangle + \langle S \rangle \tag{24}$$

in which it is assumed $\langle \mathbf{u}' \rangle = \mathbf{0}$.

Present meterological models have a large unresolved portion $\mathbf{u}'$ of the same order of magnitude as $\bar{\mathbf{u}}$ and, therefore, the term $\langle c'\mathbf{u}' \rangle$ is very large. The latter term, then, contains most of the atmospheric turbulent diffusion eddies, whose dispersion effects are orders of magnitude larger than the molecular ones. Even with a perfect meteorological model providing very detailed $\bar{\mathbf{u}}(x,y,z,t)$ information (i.e., $\bar{\mathbf{u}} \simeq \mathbf{V}$), the spatial and temporal scales of the smaller turbulent eddies are so small that a correct numerical integration of Equation 24 would be practically impossible (it would require a grid size of about 1 mm in the entire computational domain; Wyngaard, from [36]).

The output $\langle c \rangle$ provided by all Eulerian models is conceptually different from the air quality data gathered from monitoring activities. Monitoring data provide estimates of the actual concentration c (with a certain degree of error caused by the monitoring technique), while model outputs are estimates of $\langle c \rangle$ (with a certain degree of error because of the numerical and/or analytical approximations). Therefore, even during ideal conditions (i.e., with no monitoring and modeling errors), model outputs will still differ from concentration

measurements. This is often called the intrinsic (unremovable) uncertainty in air pollution dispersion modeling.

Another important point derives from the analysis of the term $\langle c'\mathbf{u}'\rangle$ in Equation 24. This term introduces three new unknowns; therefore, solving Equation 24 requires a relation between the meteorological input terms, or the average terms $\langle c\rangle$, and these three additional unknowns. The simplest approximation (phenomenological closure) is given by the so-called K-theory or gradient-transport theory in which:

$$\langle c'\mathbf{u}'\rangle = -\mathbf{K}\nabla\langle c\rangle \tag{25}$$

where $\mathbf{K}$ is a turbulent diffusivity tensor (3×3) whose elements can be inferred from meteorological measurements, or sometimes, estimated from the output of a meteorological model.

The assumption of Equation 25 has a limited applicability, especially for treating point sources in unstable conditions. More complex formulations (higher order closure schemes) have been proposed for evaluating $\langle c'\mathbf{u}'\rangle$. Lewellen and Teske [37] have developed a second-order closure dispersion model [38] for the complete equations. This model has been applied in a validation exercise against point source tracer experiment data [39]. It is not, however, currently clear if this methodology (high-order closure schemes) can provide noticeable simulation advantages with respect to other simpler techniques.

Equation 24, with the assumption of Equation 25, is generally further simplified by assuming the following: the nondiagonal terms of the tensor $\mathbf{K}$ are zero; the molecular diffusion is negligible; and c represents the concentration of a nonreactive pollutant (i.e., $\langle S\rangle = S$). With these simplifications, Equation 24 becomes the *semiempirical equation of atmospheric diffusion.*

$$\frac{\partial\langle c\rangle}{\partial t} = -\bar{\mathbf{u}}\cdot\nabla\langle c\rangle + \nabla\cdot\mathbf{K}\nabla\langle c\rangle + S \tag{26}$$

where the elements of $\mathbf{K}$ are zero, except along its main diagonal (K_{11}, K_{22}, K_{33}). Equation 26 can be integrated (analytically or numerically) if the inputs $\bar{\mathbf{u}}$, $\mathbf{K}$, and S are provided, together with initial and boundary conditions for $\langle c\rangle$.

In the case of a single source in stationary ($\partial\langle c\rangle/\partial t = 0$) emission and meteorological conditions, the source term is commonly treated as an upwind boundary condition. In this case, Equation 26 becomes simply:

$$\bar{\mathbf{u}}\cdot\nabla\langle c\rangle = \nabla\cdot\mathbf{K}\nabla\langle c\rangle \tag{27}$$

Equation 26 or 27 can be solved in two ways:

1. By analytical methods, providing exact solutions
2. By numerical methods, providing approximate solutions

These two approaches are discussed below.

Analytical Solutions

Analytical solutions are available only for extremely simplifying assumptions and cannot be generally used for actual nonstationary simulations. The problem of finding a satisfactory analytical solution for Equation 27 with reflecting boundaries has been particularly debated

([40–43]). A recent paper [44] provides a complete set of the analytical solutions to Equation 27, with or without reflection from the top of the PBL.

Numerical Solutions

Numerical methods allow the computation of approximate solutions of Equations 26 and 27 using different integration techniques, such as:

1. Finite-difference methods
2. Finite-element methods
3. Spectral methods
4. Boundary-element methods
5. Particle methods

Finite-difference methods [45] are the oldest technique. Although they possess several disadvantages, they still represent the major and most applied (and best understood) numerical tool for this type of application. However, the finite-difference approximation of the advection term $\bar{\mathbf{u}} \cdot \nabla < c >$ always produces a diffusion-type error (often a very large error) that artificially increases the diffusion rates in the simulated concentration output.

While analytical solutions require special, simplified functional forms for the **K** terms (i.e., power laws of the altitude z), numerical solutions can accommodate virtually any functional relationship. Several of these functions have been proposed for evaluating K_H, the horizontal eddy diffusivity (which assumes $K_{11} = K_{22} = K_H$ for any wind direction angle with the x-axis), and K_z ($= K_{33}$), the vertical eddy diffusivity. McRae et al. [46] give a complete set of K_H and K_z functions, and more information on this topic can be found in [47].

GAUSSIAN MODELS

Gaussian models are generally treated as a category of their own. However, Gaussian formulas can be derived from both Eulerian and Lagrangian approaches, even though, as depicted in Figure 4, Gaussian models, in their most general form, should be seen as a special simplification of the Lagrangian approach.

The Gaussian Approach

The Gaussian plume model is the most common air pollution model. It is based on a simple formula that describes the three-dimensional concentration field generated by a point source under stationary meteorological and emission conditions as (see Figure 5):

$$c = \frac{Q}{2\,\pi\sigma_h\sigma_z\,|\,\bar{\mathbf{u}}\,|} \exp\left[-\frac{1}{2}\left(\frac{\Delta cw}{\sigma_h}\right)^2\right] \exp\left[-\frac{1}{2}\left(\frac{z_s + \Delta h - z_r}{\sigma_z}\right)^2\right] \tag{28}$$

where $c(\mathbf{s}, \mathbf{r})$ is the concentration at the receptor $\mathbf{r} = (x_r, y_r, z_r)$ due to the emissions at the source $\mathbf{s} = (x_s, y_s, z_s)$; Q is the pollutant mass emission rate; $\sigma_h(j_h, d)$ and $\sigma_z(j_z, d)$ are the standard deviations (horizontal and vertical) of the plume concentration spatial distribution (often σ_h is referred to as σ_y); j_h and j_z are the horizontal and vertical turbulence states (further discussed below); d is the downwind distance of the receptor from the source:

$$d = [(\mathbf{r} - \mathbf{s}) \cdot \bar{\mathbf{u}}]/|\,\bar{\mathbf{u}}\,| \tag{29}$$

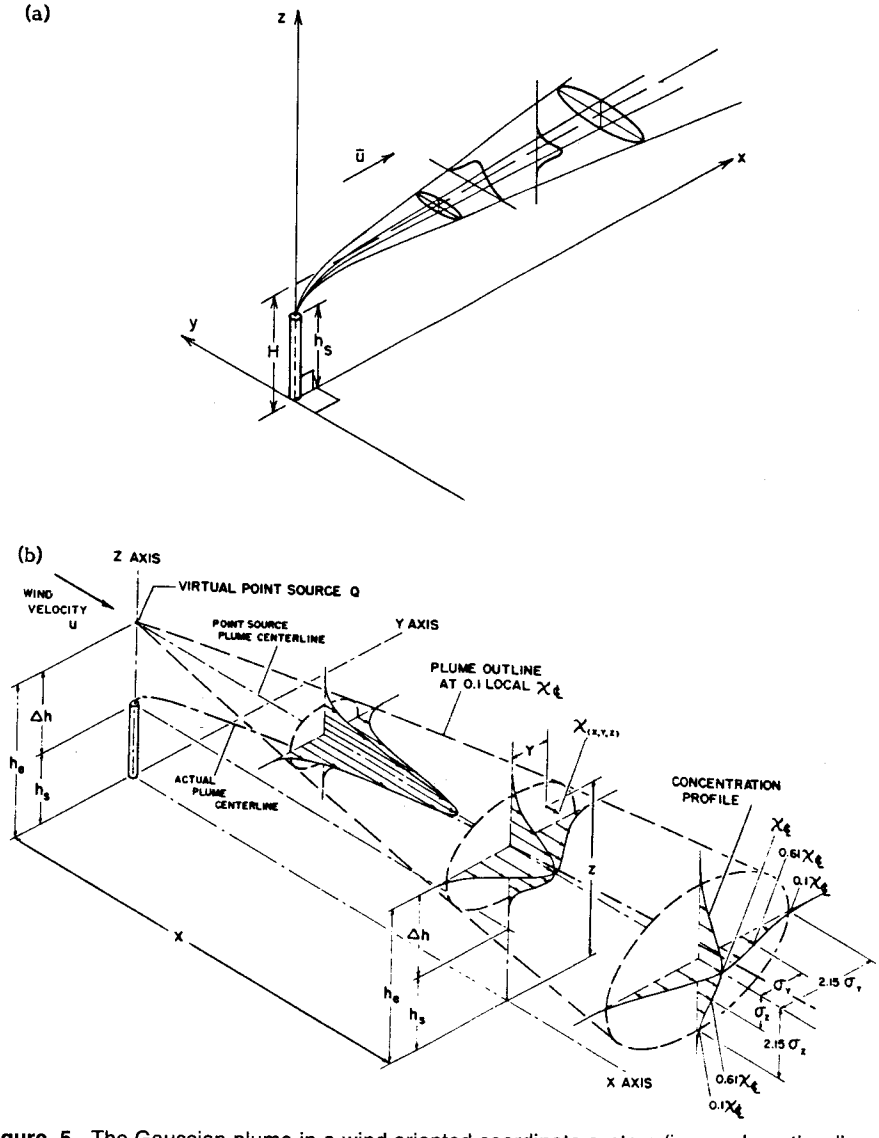

Figure 5. The Gaussian plume in a wind-oriented coordinate system (i.e., x along the direction of u): (a) an elevated source location in (0,0,H) (from [55a]. Reprinted with permission from John Wiley Le Sons, Inc.); (b) three-dimensional concentration profiles. (From Strom in [24]. Reprinted with permission from Academic Press.)

$\bar{\mathbf{u}}$ is the average wind velocity vector ($\bar{u}_x$, $\bar{u}_y$, $\bar{u}_z$) at the emission height; Δ_{cw} is the crosswind distance between the receptor and source (i.e., between the receptor and the plume centerline):

$$\Delta_{cw} = (|\mathbf{r} - \mathbf{s}|^2 - d^2)^{1/2} \tag{30}$$

and $\Delta h(d)$ is the emission plume rise. Equation 28 is applied for $d > 0$; if $d \leq 0$, then $c = 0$.

Equation 28 refers to a stationary state (c is not a function of time), uses meteorological conditions (wind and turbulence states) that must be considered homogeneous and stationary in the modeled area (i.e., between **s** and **r**), and cannot work in calm conditions where $|\bar{\mathbf{u}}| \to 0$. However, the simplicity of the Gaussian approach, its relative ease of use with clearly measurable meteorological parameters, and, especially, the elevation of this methodology to the quantitative decision-controlling level [48] have stimulated research aimed at removing some of its limitations in treating the complex situations of the real world.

Equation 28 is generally written in the form:

$$c = \frac{Q}{2\,\pi\sigma_h\sigma_z\bar{u}} \exp\left[-\frac{1}{2}\left(\frac{y_r}{\sigma_y}\right)^2\right] \exp\left[-\frac{1}{2}\left(\frac{h_e - z_r}{\sigma_z}\right)^2\right] \tag{31}$$

where $\bar{u}$ = average wind speed
h_e = effective emission height ($h_e = z_s + \Delta h$)

and σ_y replaces σ_h. Here, a wind-oriented coordinate system is also used (as in Figure 5). Equation 31 can be derived in several ways from different assumptions and can be justified by semi-empirical considerations, as illustrated in Figure 6, where both instantaneous and average concentration distributions are exemplified. Even though instantaneous plume concentrations are quite irregular, a sufficiently long averaging time (e.g., one hour) generates, in many cases, bell-shaped concentration distributions that can be well approximated by the Gaussian distribution in both the horizontal and (to a lesser degree) the vertical.

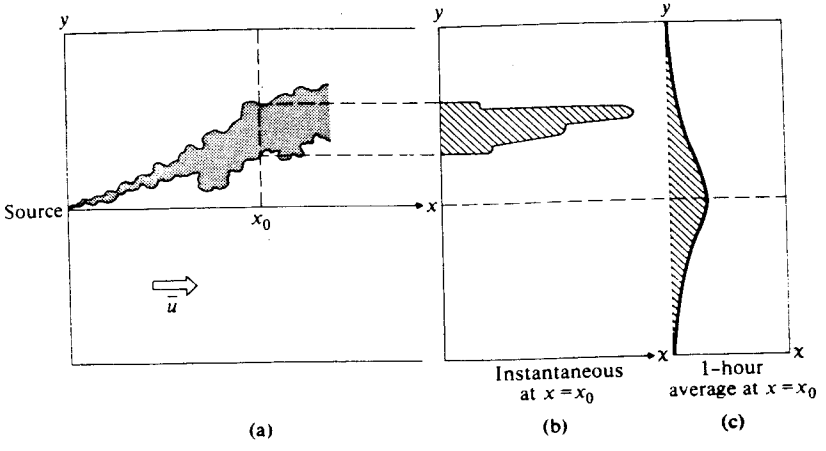

Figure 6. (a) Instantaneous top view of a plume; (b) instantaneous horizontal profile of the plume concentration x along a transverse direction at some distance downwind from the source; (c) one-hour average profile for the same downwind distance from [48a]. Reprinted with permission from Addison-Wesley Publishing Co.

The Calculation of σ_y and σ_z

Concentrations computed by Equation 31 depend strongly on the choices of σ_y and σ_z, which represent a major source of uncertainty for all Gaussian model applications.

The Nondimensional S_y and S_z Functions for the Gaussian Model

Pasquill [49] suggested the following relationships for plume sigmas, which are consistent with Taylor's [50] statistical theory of diffusion:

$$\sigma_y = \sigma_v \, t \, S_y(t/T_L) \tag{32}$$

$$\sigma_z = \sigma_w \, t \, S_z(t/T_L) \tag{33}$$

where σ_v and σ_w are the standard deviations of the cross-wind and vertical wind vector components (which can be either measured or estimated by semi-empirical formulas), and S_y and S_z are universal functions of the diffusion (or travel) time t and the Lagrangian time scale T_L.

Draxler [51] rewrote the above equations as:

$$\sigma_y = \sigma_\theta \, x \, S_y(t/T_i) \tag{34}$$

$$\sigma_z = \sigma_\phi \, x \, S_z(t/T_i) \tag{35}$$

where σ_θ and σ_ϕ = standard deviations of wind vector azimuth and elevation angles
x = downwind distance

and T_i is a normalization factor ($T_i = 1.64 \, T_L$ is the time required for S_y or S_z to become equal to 0.5; S_y and S_z are always equal to 1 for t = 0).

Draxler [51] also analyzed available dispersion data, giving a preliminary evaluation of the specific forms of S_y and S_z and determining T_i. Pasquill [52] tabulated S_y as a universal function of x only. These tabulated values were then reformulated by Irwin [53] as:

$$S_y(x) = (1 + 0.0308 \, x^{0.4548})^{-1} \text{ for } x \leq 10^4 \text{ m} \tag{36}$$

$$S_y(x) = 0.333 \, (10{,}000/x)^{0.5} \text{ for } x > 10^4 \text{ m} \tag{37}$$

Currently, the above formulation of S_y is generally accepted as the best way to determine σ_y and has been recommended by the American Meteorological Society Workshop on Stability Classification Schemes and Sigma Curves [54]. Phillips and Panofsky [55], however, suggested a new S_y formulation that provides a better fit of experimental data for small x and is consistent with inertial-subrange theory, namely:

$$S_y = 0.617 \left[\frac{T_i}{t} - \frac{(T_i/t)^2}{5.25} \ln \left(1 + 5.25 \, \frac{t}{T_i} \right) \right]^{1/2} \tag{38}$$

The evaluation of S_z is still quite uncertain. Irwin [53] provided a preliminary universal function S_z and recommended its interim use until more field data permit the evaluation of a more accurate scheme. In unstable conditions, his S_z function depends upon the depth of the mixing layer, the diffusion time, the effective release height, the surface friction velocity, and the Monin-Obukov length. Draxler [51] derived, under neutral and stable conditions:

$$S_z = [1 + 0.9\ (t/T_o)^{1/2}]^{-1} \quad \text{for } z_s < 50 \text{ m} \tag{39}$$

$$S_z = [1 + 0.945\ (t/T_o)^{0.8}]^{-1} \quad \text{for } z_s \geq 50 \text{ m} \tag{40}$$

in which the characteristic time $T_o \simeq 50$ s.

Semi-Empirical σ Calculations

Several schemes are available that allow the computation of σ_y and σ_z from the downwind distance x and the atmospheric stability class (i.e., an empirical classification of the horizontal and vertical atmospheric turbulence states j_h and j_z). The stability class can be computed using the Pasquill or Turner methods (see Tables 1 and 2) or from measurements of σ_θ, σ_w, or $\Delta T/\Delta z$, as illustrated in Tables 3 and 4. Tracer experiments, however, have shown that horizontal and vertical diffusion rates are often related to different stability categorizations and, therefore, a "split-sigma" approach should generally be adopted, in which σ_y and σ_z dynamics are evaluated as functions of "horizontal" and "vertical" stability classes, respectively. Results indicate that σ_θ measurements provide a good estimate of the horizontal stability, while vertical temperature gradient data seem appropriate for identifying the vertical stability class.

Table 1
Pasquill Dispersion Classes [55a]

Insolation/Cloud Cover		Surface Wind Speed (m/s)				
		<2.0	2 to <3	3 to <5	5 to <6	≥6
Day	Strong Insolation	A	A–B	B	C	C
	Moderate Insolation	A–B	B	B–C	C–D	D
	Slight Insolation	B	C	C	D	D
Day or Night	Overcast	D	D	D	D	D
Night	Thin overcast or ≥0.5 cloud cover	—	E	D	D	D
	≤0.4 cloud cover	—	F	E	D	D

* *Reprinted with permission from John Wiley & Sons, Inc.*

Notes: 1. Strong insolation corresponds to a solar elevation angle of 60° or more above the horizon. Slight insolation corresponds to a solar elevation angle of 15° to 35°.

2. Pollutants emitted under clear nighttime skies with winds less than 2.0 m/s, more recently defined to be class G, may be subject to unsteady meandering which renders the prediction of concentrations at downwind locations unreliable.

* *A, very unstable; B, unstable; C, slightly unstable; D, neutral; E, slightly stable; F, stable; G, very stable.*

Table 2
Definition of Turner Classes [1]*

Wind Speed (knots)	Net Radiation Index						
	4	3	2	1	0	− 1	− 2
0–1	1	1	2	3	4	6	7
2–3	1	2	2	3	4	6	7
4–5	1	2	3	4	4	5	5
6	2	2	3	4	4	5	6
7	2	2	3	4	4	4	5
8–9	2	3	3	4	4	4	5
10	3	3	4	4	4	4	5
11	3	3	4	4	4	4	4
≥ 12	3	4	4	4	4	4	4

Solar Altitude (a)	Insolation	Insolation Class Number
60° < a	Strong	4
35° < a < 60°	Moderate	3
15° < a < 35°	Weak	2
a ≤ 15°	Very Weak	1

* *Reprinted with permission from John Wiley & Sons, Inc.*

Definitions of Net Radiation Index

1. If the total cloud cover is 10/10 and the ceiling is less than 7000 ft, use net radiation index equal to 0 (whether day or night).
2. For nighttime (between sunset and sunrise):
   (a) If total cloud cover ≤ 4/10, use net radiation index equal to − 2.
   (b) If total cloud cover > 4/10, use net radiation index equal to − 1.
3. For daytime:
   (a) Determine the insolation class number as a function of solar altitude from Table 6.4.
   (b) If total cloud cover ≤ 5/10, set the net radiation index above equal to the insolation class number.
   (c) If cloud cover > 5/10, modify the insolation class number by the following six steps.
      (1) Ceiling < 7000 ft, subtract 2.
      (2) Ceiling ≥ 7000 ft but < 16,000 ft, subtract 1.
      (3) Total cloud cover equals 10/10, subtract 1. (This will only apply to ceilings ≥ 7000 ft since cases with 10/10 coverage below 7000 ft are considered in item 1 above.)
      (4) If insolation class number has not been modified by steps (1), (2), or (3) above, assume modified class number equal to insolation class number.
      (5) If modified insolation class number is less than 1, let it equal 1.
      (6) Use the net radiation index in Table 6.4 of [1] corresponding to the modified insolation class number.

Since urban areas do not become as stable in the lower layers as nonurban areas, stability classes computed as 6 and 7 by this system are called class 5 in urban areas.

* *1: very unstable; 2: unstable; 3: slightly unstable; 4: neutral; 5: slightly stable; 6: stable; 7: very stable.*

Table 3
Classification of Atmospheric Stability [55b]

Stability Classification	Pasquill Categories	σ_θ** (degrees)	ΔT Temperature Change with Height (°C 100 m^{-1})
Extremely unstable	A	25.0	< -1.9
Moderately unstable	B	20.0	-1.9 to -1.7
Slightly unstable	C	15.0	-1.7 to -1.5
Neutral	D	10.0	-1.5 to -0.5
Slightly stable	E	5.0	-0.5 to 1.5
Moderately stable	F	2.5	1.5 to 4.0
Extremely stable	G	1.7	>4.0

* *Reprinted with permission from Pergamon Journals, Inc.*
** *Standard deviation of horizontal wind direction fluctuation over a period of 15 min–1 h. The values shown are averages for each stability classification.*

Table 4
Classification of Atmospheric Stability (Adapted from [63])

Pasquill Stability Category	Standard Deviation of the Horizontal Wind Direction Fluctuations (in degrees)	Standard Deviation of the Vertical Wind Direction Fluctuations (in degrees)
A	Greater than 22.5°	Greater than 11.5°
B	17.5° to 22.5°	10.0° to 11.5°
C	12.5° to 17.5°	7.8° to 10.0°
D	7.5° to 12.5°	5.0° to 7.8°
E	3.8° to 7.5°	2.4° to 5.0°
F	Less than 3.8°	Less than 2.4°

After the computation of the stability class, σ_y and σ_z can be computed at a certain downwind distance x by choosing one of the several available formulas:

1. Pasquill-Gifford sigmas [56], presented graphically in [57] and analytically in [58] as:

$$\sigma_y(x) = \frac{k_1\, x}{[1 + (x/k_2)]^{k_3}} \tag{41}$$

$$\sigma_z(x) = \frac{k_4\, x}{[1 + (x/k_2)]^{k_5}} \tag{42}$$

where the constants k_1, k_2, k_3, k_4, k_5 are given in Table 5.

The foregoing σ_y, σ_z values were derived [59] primarily from a diffusion experiment in flat terrain (with roughness length $z_o \simeq 0.03$ m) in which a nonbuoyant tracer gas was released near the surface and measured (three-minute averages) downwind up to a distance of 800 m from the source. Pasquill-Gifford sigmas are the most used formulation for U.S. EPA regulatory modeling applications.

Table 5
Values of the Constants in Equations 41 and 42 (Adapted from [58])

Stability Class	k_1	k_2	k_3	k_4	k_5
A	0.250	927	0.189	0.1020	−1.918
B	0.202	370	0.162	0.0962	−0.101
C	0.134	283	0.134	0.0722	0.102
D	0.0787	707	0.135	0.0475	0.465
E	0.0566	1,070	0.137	0.0335	0.624
F	0.0370	1,170	0.134	0.0220	0.700

Table 6
Coefficients a, b for Equation 43 (Adapted from [59])

Gustiness Category	σ_y		σ_z	
	a	b	a	b
B_2	0.40	0.91	0.41	0.91
B_1	0.36	0.86	0.33	0.86
C	0.32	0.78	0.22	0.78
D	0.31	0.71	0.06	0.71

Table 7
Relation between the "Gustiness" Category and the Pasquill Class (Adapted from [59])

Pasquill Class	Gustiness Category
A	B_2 (Very unstable)
B	B_1 (Unstable)
C	B_1 (Unstable)
D	C (Neutral)
E	C/D (Neutral/stable)
F	D (Stable)

2. Brookhaven sigmas [60], in which a power law function is assumed for both σ_y and σ_z; i.e.:

$$\sigma = a\ x^b \tag{43}$$

The coefficients a and b are given in Table 6 for each "gustiness" category. Table 7 illustrates the relation between the "gustiness" category and the Pasquill classes.

This scheme was derived from elevated releases (108 m) over a rough surface ($z_o \simeq 1$ m), with concentrations measured up to a few kilometers downwind.

3. Briggs sigmas [61], in urban and rural versions, provide an interpolation scheme that agrees with Pasquill-Gifford in the downwind range from 100 m to 10 km, except that

Table 8
The Briggs Sigma Functions for (a) Urban and (b) Rural Conditions (from [61a])

(a)

Pasquill type	σ_y, m	σ_z, m
A–B	$0.32x\ (1 + 0.0004x)^{-0.5}$	$0.24x\ (1 + 0.001x)^{0.5}$
C	$0.22x\ (1 + 0.0004x)^{-0.5}$	$0.20x$
D	$0.16x\ (1 + 0.0004x)^{-0.5}$	$0.14x\ (1 + 0.0003x)^{-0.5}$
E–F	$0.11x\ (1 + 0.0004x)^{-0.5}$	$0.08x\ (1 + 0.0015x)^{-0.5}$

(b)

Pasquill type	σ_y, m	σ_z, m
A	$0.22x\ (1 + 0.0001x)^{-0.5}$	$0.20x$
B	$0.16x\ (1 + 0.0001x)^{-0.5}$	$0.12x$
C	$0.11x\ (1 + 0.0001x)^{-0.5}$	$0.08x\ (1 + 0.0002x)^{-0.5}$
D	$0.08x\ (1 + 0.0001x)^{-0.5}$	$0.06x\ (1 + 0.0015x)^{-0.5}$
E	$0.06x\ (1 + 0.0001x)^{-0.5}$	$0.03x\ (1 + 0.0003x)^{-1}$
F	$0.04x\ (1 + 0.0001x)^{-0.5}$	$0.16x\ (1 + 0.0003x)^{-1}$

σ_z values for A and B stability approximate the B_2 and B_1 Brookhaven curves. Table 8 gives the Briggs sigmas. The urban Briggs sigmas (also called McElroy-Pooler sigmas) were derived from several urban dispersion experiments with low-level tracers [62]. The U.S. EPA recommends these sigma values as those for dispersion simulation in urban areas [63].

Reflection Terms

The basic Gaussian formula is often used with the assumption of total or partial concentration reflection at the surface. With ground reflection, the last term in Equation 31 becomes:

$$S(z_r) = \exp\left[-\frac{1}{2}\left(\frac{h_e - z_r}{\sigma_z}\right)^2\right] + r_g \exp\left[-\frac{1}{2}\left(\frac{h_e + z_r}{\sigma_z}\right)^2\right] \tag{44}$$

where r_g is the ground reflection coefficient ($r_g = 1$, total reflection, is generally assumed). For receptors at the ground ($z_r = 0$) with $r_g = 1$, Equation 44 becomes:

$$S(0) = 2 \exp\left[-\frac{1}{2}\left(\frac{h_e}{\sigma_z}\right)^2\right] \tag{45}$$

which, for ground-level nonbuoyant sources (i.e., $h_e = 0$), gives:

$$S(0) = 2 \tag{46}$$

If the plume is emitted within the PBL, the plume can also be reflected at the top, z_i, of the PBL with a reflection coefficient r_i ($r_i = 1$, total reflection, is generally assumed). The presence of a second reflecting barrier causes multiple reflections and, therefore, with the assumption $r_g = r_i = 1$, we obtain:

$$S(z_r) = \sum_{j=0,\pm1,\pm2,\ldots} \left\{ \exp\left[-\frac{1}{2}\left(\frac{z_r + 2jz_i - h_e}{\sigma_z} \right)^2 \right] + \exp\left[-\frac{1}{2}\left(\frac{z_r + 2jz_i + h_e}{\sigma_z} \right)^2 \right] \right\} \tag{47}$$

In some cases, Equation 47 shows a slow convergence. To avoid excessive computations, Yamartino [64] proposed an efficient analytical method for approximating Equation 47 with an error $\leq 1.3\%$.

Dynamic Applications of the Gaussian Formula

The Segmented Plume Model

The Gaussian steady-state formula described in Equation 28 or 31 is valid only during fairly stationary and homogeneous transport conditions (e.g., $\bar{u} \geq 1$ m/s). In order to treat time-varying transport conditions and, especially, changes in wind direction, several authors have developed and used a segmented Gaussian plume (e.g., [65–67]). In the segmented plume approach, the plume is broken up into independent elements (plume segments or sections) whose initial features and time dynamics are a function of time-varying emission conditions and the local time-varying meteorological conditions encountered by the segments along their motion.

The segmented plume features are illustrated in Figure 7, which shows a plan view (solid lines) of a segmented plume encountering a progressive change of wind direction along its trajectory. Segments are sections of a Gaussian plume. Each segment, however, generates a concentration field that is still computed by Equation 28 and that represents the contribution of the entire virtual plume passing through that segment, as illustrated by the dotted lines in Figure 7. Therefore, only one segment (the closest) affects the concentration computation at each receptor, although the occurrence of a 180° wind direction change can create a condition where the contribution of two segments (that is, two virtual plumes) should be superimposed at some receptors.

Puff Models

Like segmented models, puff models (e.g., [68, 69]) have been developed to treat nonstationary nonhomogeneous emission and dispersion conditions. Puff methods, however, have the additional advantage of being able, at least theoretically, to simulate calm or low wind conditions.

The Gaussian puff model assumes that each pollutant emission of duration Δt injects into the atmosphere a mass $\Delta M = Q\Delta t$, where Q is the time-varying emission rate. The center of the puff containing the mass ΔM is advected according to the local time-varying wind vector. If, at time t, the center of a puff is located at $\mathbf{p}(t) = (x_p, y_p, z_p)$, then the concentration Δc due to that puff at the receptor $\mathbf{r} = (x_r, y_r, z_r)$ can be computed using the basic Gaussian puff formula:

$$\Delta c = \frac{\Delta M}{(2\pi)^{3/2}\,\sigma_h^2 \sigma_z} \exp\left[-\frac{1}{2}\left(\frac{x_p - x_r}{\sigma_h} \right)^2 \right] \cdot \exp\left[-\frac{1}{2}\left(\frac{y_p - y_r}{\sigma_h} \right)^2 \right] \exp\left[-\frac{1}{2}\left(\frac{z_p - z_r}{\sigma_h} \right)^2 \right] \tag{48}$$

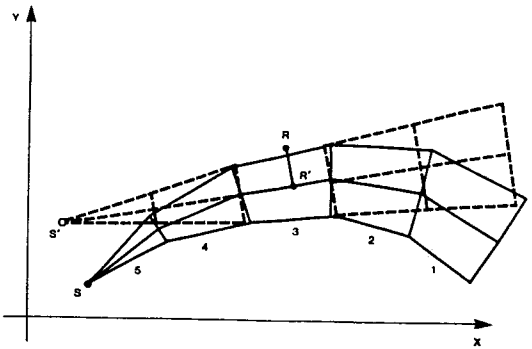

Figure 7. Computation of the concentration at the receptor R generated by the segmented plume (solid lines). The computation is performed by evaluating the contribution of the virtual plume (dotted lines) from the virtual source S′ passing through the closest segment (number 3) to the receptor R [73]. Reprinted with permission from Pergamon Journals, Inc.

which is often expanded to incorporate reflection and deposition/decay terms. The analytical integration of Equation 48 in stationary, homogeneous transport conditions, gives the Gaussian plume formula of Equation 31.

Equation 48 requires the evaluation of the horizontal (σ_h) and vertical (σ_z) dynamics of each puff's growth. The total concentration in a receptor at time t is computed by adding the contribution Δc from all existing puffs generated by all sources. Note that Equation 48 differs from Equation 31 mainly because an extra horizontal diffusion term has been substituted for the transport term with the consequent disappearance of the wind speed $\bar{u}$. In a puff model, the wind speed directly affects the concentration computation only by controlling the density of puffs in the region (that is, the lower the wind speed, the closer a puff is to the next one generated by the same source). Therefore, at least in theory, a puff model can handle calm or low-wind conditions, and this approach represents the most advanced and powerful application of the Gaussian formula.

Several studies have discussed the puff modeling approach in detail, improving its application features. Algorithms have been proposed and evaluated for incorporating wind shear effects [70]. Virtual distance [71] and virtual age [72] computations have been defined for evaluating the σ_h and σ_z dynamics of the puff. Puff merging [71] or puff splitting [72] have been incorporated for performing cost-effective simulations with relatively large Δt (for example, 5–10 minutes). An empirical method has been derived [72] for evaluating the puff's σ_h and σ_z growth during calm or low-wind conditions as a function of currently available σ functions during transport conditions.

Mixed Segment-Puff Methodology

A new mixed methodology has recently been proposed by Zannetti [73]. It combines the advantages of both the segment and puff approaches for realistic and cost-effective simulation of short-term plume dispersion phenomena using the Gaussian formula.

According to this method, pollutant dynamics are described by the temporal evolution of plume elements, treated as segments or puffs according to their size. While the segments provide a numerically fast simulation during transport conditions, the puffs allow a proper simulation of calm or low-wind situations.

LAGRANGIAN DISPERSION MODELS

The Lagrangian Approach

The fundamental Lagrangian equation for atmospheric dispersion of a single pollutant species, as was illustrated in Figure 4, is:

$$<c(\mathbf{r}, t)> = \int_{-\infty}^{t}\int \int p(\mathbf{r}, t \mid \mathbf{r}', t')\, S(\mathbf{r}', t')\, d\mathbf{r}'\, dt' \tag{49}$$

where the integration in space is performed over the entire atmospheric domain; $<c(\mathbf{r}, t)>$ is the ensemble average concentration at $\mathbf{r}$ at time t; $S(\mathbf{r}', t')$ is the source term (mass volume^{-1} time^{-1}); and $p(\mathbf{r}, t \mid \mathbf{r}', t')$ is the probability density function (volume $^{-1}$) that an air parcel moves from $\mathbf{r}'$ at t' to $\mathbf{r}$ at t, where, for any $\mathbf{r}'$ and $t > t'$:

$$\int p(\mathbf{r}, t \mid \mathbf{r}', t')\, d\mathbf{r} = 1 \tag{50}$$

The expression in Equation 50 can be less than one when chemical or deposition phenomena are considered; otherwise mass conservation always requires the value to be equal to one. For a primary pollutant, $S(\mathbf{r}', t') > 0$ only at points $\mathbf{r}'$ where the pollutant is released (e.g., exit point of stacks). For a secondary pollutant, $S(\mathbf{r}', t')$ can be nonzero virtually anywhere. For both primary and secondary pollutants however, Equation 50, which represents mass conservation, must be satisfied.

Since it is often difficult to evaluate the entire emission "history" $S(\mathbf{r}', t')$ for $-\infty \leq t' \leq t$, Equation 49 can be rewritten as:

$$<c(\mathbf{r}, t)> = \int p(\mathbf{r}, t \mid \mathbf{r}', t_o) <c(\mathbf{r}', t_o)> d\mathbf{r}' + \int_{t_o}^{t}\int p(\mathbf{r}, t \mid \mathbf{r}', t') S(\mathbf{r}', t')\, d\mathbf{r}'\, dt' \tag{51}$$

in which only the contribution of the sources during $t_o \leq t' < t$ needs to be included, since the first integral term accounts for the source contribution before t_o. However, Equation 51 requires some estimate of the average concentration $<c>$ at t_o throughout the computational domain.

The key parameter in the preceding equations is the probability density function p, which, for nonreactive pollutants, is a function of only the meteorology and the type of pollutant. Equations 49 or 51 are the most rigorous description of transport and diffusion processes, expressed in a probabilistic notation.

Different assumptions concerning the probability density function p allow the derivation of both Gaussian equations and the K-theory equation, as was illustrated in Figure 4. In particular, Seinfeld [74] shows that all Gaussian plume and puff formulas can be derived from the Lagrangian Equation 49 under the following simplifying assumptions:

1. Turbulence is stationary and homogeneous; i.e.:

$$p(\mathbf{r}, t \mid \mathbf{r}', t') = p(\mathbf{r} - \mathbf{r}', t - t') \tag{52}$$

2. p obeys a multi-dimensional normal distribution; i.e.:

$$p(\mathbf{r} - \mathbf{r}', t - t') = \frac{1}{(2\pi)^{3/2} \mid \mathbf{P} \mid^{1/2}} \exp\left[-\zeta^{T}\mathbf{P}^{-1}\zeta/2\right] \tag{53}$$

where each element P_{ij} of the 3 x 3 matrix $\mathbf{P}$ is:

$$P_{ij} = <\zeta_i \zeta_j> \tag{54}$$

and the "displacements" ζ_i are:

$$\zeta_i = [\mathbf{r} - \mathbf{r}']_i - [<\mathbf{r} - \mathbf{r}'>]_i \tag{55}$$

in which i indicates the space component (x, y, or z, for i = 1, 2, or 3, respectively).

3. The term $<\mathbf{r} - \mathbf{r}'>$ is the average displacement, which is assumed to be due only to the average (deterministic) wind $\bar{\mathbf{u}}$.
4. $P_{ij} = 0$, for $i \neq j$.

Several types of models can be classified as Lagrangian:

1. Lagrangian box, or trajectory models, which are used for photochemical simulations and, therefore, will not be further discussed.
2. Gaussian segmented plume models, which were discussed earlier.
3. Gaussian puff models, also discussed earlier.
4. Particle models, which are fully discussed below.

Particle Models

Particle modeling is the most recent and most powerful computational tool for the numerical discretization of a physical system. It has been particularly successful in a wide spectrum of applications [75] that range from the atomic scale (electron flow in semiconductors, molecular dynamics) to the astronomical scale (galaxy dynamics), with other important applications to plasma and turbulent fluid dynamics. Using particle models, the temporal evolution of a physical system is described by the dynamics of a finite number of computational (fictitious) particles.

Transport terms, whose correct numerical treatment is very difficult with Eulerian (grid) models, are handled in a straightforward manner by particle models, since particles simply move following the main flow; for this reason, they are often called Lagrangian particles.

Particle models can be purely deterministic or can possess statistical (random) characteristics. In the first case, particle motion is generated by forces originated from particle interactions and/or potential fields. In the second case, semirandom pseudovelocities are generated using Monte-Carlo computer techniques. In the first case, the simulation of particle time evolution is unique. In the second case, Monte Carlo techniques produce semirandom "perturbations" and, therefore, the dynamics of each particle represent just one realization of an infinite set of possible solutions. Particle models using Monte-Carlo methods are particularly important since, in several applications, they allow each particle to move independently of the others. Thus, they provide a computational algorithm that is generally faster than the corresponding deterministic computations, where interactions between neighboring particles need to be computed.

In air pollution applications using Lagrangian particle methods, emitted gaseous material is characterized by particles and each particle is "moved" at each time step by a pseudo velocity $\mathbf{u}_e$, which takes into account the three basic dispersion components: the transport due to the mean fluid velocity, the (seemingly) random turbulent fluctuations of wind components (both horizontal and vertical), and the molecular diffusion (if not negligible). In mathematical notation, we can define this pseudo-velocity as:

$$\mathbf{u}_e = \bar{\mathbf{u}}_e + \mathbf{u}'_e \tag{56}$$

where $\bar{\mathbf{u}}_e \simeq \bar{\mathbf{u}}$, i.e., the best estimate of the average Eulerian wind vector (transport) at the particle location, and $\mathbf{u}'_e$ is a "diffusivity velocity." In other words, $\bar{\mathbf{u}}_e$ (a smoothly variable term) represents our deterministic understanding of the average transport process, based on Eulerian wind measurement interpolation or provided by a meteorological model, while $\mathbf{u}'_e$ is an artificial numerical perturbation, which is related to the turbulence intensities of those eddies that are not included in the $\bar{\mathbf{u}}_e$ field. It must be noted that the meteorological input above refers to the statistical description of the fluctuating component $\mathbf{u}'_e$, which should not be seen as an *intrinsic* description of turbulence, but as a description of the *unresolved* com-

ponent of the wind flow, i.e., the portion $\mathbf{u}'_e$ of the flow that is not contained in the average flow $\bar{\mathbf{u}}_e$.

Since, in Equation 56, $\bar{\mathbf{u}}_e$ is assumed to be known from measurements and/or meteorological model outputs, computing $\mathbf{u}'_e$ is the key problem of Lagrangian particle modeling. Two fundamental approaches can be followed: the deterministic and the statistical.

The Deterministic Computation of $\mathbf{u}'_e$

A typical example of the deterministic approach is given by the particle-in-cell method [76], where, after some manipulation of the K-theory diffusion equation, we obtain:

$$\mathbf{u}'_e = \left(-\frac{K}{c}\right) \nabla c \tag{57}$$

where K is the eddy diffusion coefficient and c the concentration, computed from the number of particles in a unit volume (or a cell) at the particle location. This method requires partitioning the computational domain into cells in order to calculate c. It is able to duplicate K-theory dispersion with the important feature of decreasing the numerical advection errors otherwise produced by finite-difference solutions. Using this method, the motion of a single particle will be affected by the time-varying concentration field c, i.e., by the positions of the other particles.

The Statistical Computation of $\mathbf{u}'_e$

The statistical approach (Monte Carlo-type models) certainly seems to be more flexible and appealing than the deterministic approach. According to the statistical approach, $\mathbf{u}'_e$ is a semirandom component computed by manipulating computer-generated random numbers. It is generally assumed that, for a particle moving during the interval from t_1 to t_2:

$$\mathbf{u}'_e(t_2) = \mathbf{R}_e(\Delta t)\ \mathbf{u}'_e(t_1) + \mathbf{u}''_e(t_2) \tag{58}$$

where* $\mathbf{R}_e(\Delta t)$ contains the autocorrelations with lag $\Delta t = t_2 - t_1$ of the $\mathbf{u}'_e$ components, and $\mathbf{u}''_e$ is a purely random vector that will be discussed further below.

Equation 58 is a key formula for statistically computing $\mathbf{u}'_e$. It is a recursive sum of two terms—the first is a function of the "previous" $\mathbf{u}'_e$ of the same particle, and the second is randomly generated. Since Equation 58 is computed independently for each particle, two eventually coincident particles at t_1 will have, in general, different displacements, even if their past "history" is exactly the same. Using this approach, the motion of a particle is not affected by the position of the other particles and, therefore, this numerical algorithm is extremely fast, since no interacting forces need to be computed.

Application of Equation 58 requires the estimate of the initial $\mathbf{u}'_e(t_o)$ for each particle at its generation time t_o (often assumed to be a zero vector) and the dynamic computation of $\mathbf{R}_e$ and $\mathbf{u}''_e$.

Due to the Lagrangian nature of $\mathbf{u}_e$, $\mathbf{R}_e$ has been often identified with $\mathbf{R}_L$, the autocorrelations of the Lagrangian wind vector $\mathbf{u}_L$. $\mathbf{R}_L$ can be related to Lagrangian turbulence time scales, for example, by:

$$\mathbf{R}_L(\Delta t) = \exp\left(-\Delta t/\mathbf{T}_L\right) \tag{59}$$

where $\mathbf{T}_L$ contains the two horizontal and the one vertical Lagrangian time scales. Generally, Lagrangian measurements of $\mathbf{T}_L$ (or $\mathbf{R}_L$ directly) are not available, but empirical relations

* In this formula (and the following ones in this section) each component of the vector on the left side is computed using only the corresponding component of each vector in the right side (componentwise notation).

have been proposed (e.g., Hanna, in [36]) to estimate $\mathbf{T_L}$ from Eulerian meteorological measurement.

Assuming that $\mathbf{u_e''}$ is a purely random vector with zero-mean, normally-distributed independent components, it is completely characterized by $\boldsymbol{\sigma}_{\mathbf{u}''}$, i.e., the standard deviations of its components. In this case, taking the variances of Equation 58:

$$\boldsymbol{\sigma}_{\mathbf{u}''} = \boldsymbol{\sigma}_{\mathbf{u}''} \, [1 - \mathbf{R}_e^2(\Delta t)]^{1/2} \tag{60}$$

whose calculation requires the knowledge of $\boldsymbol{\sigma}_{\mathbf{u}}$, the standard deviations of $\mathbf{u_e'}$ which, again, can be approximated by the standard deviations of available Eulerian wind measurements.

Using the standard deviations $\boldsymbol{\sigma}_{\mathbf{u}''}$ computed by Equation 60, it is easy, with commonly available Monte-Carlo computer programs, to generate each particle's $\mathbf{u_e''}$ term for use in Equation 58.

$\mathbf{R_e}$ and $\boldsymbol{\sigma}_{\mathbf{u}}$ are, in general, time-dependent (but assumed constant between t_1 and t_2) and space-dependent, especially z-dependent. Therefore, they can fully use a three-dimensional meteorological input and can, at least theoretically, simulate extremely complex atmospheric diffusion conditions, which are impossible to treat with other numerical schemes.

Several current models are based on Equation 58 in which the components of $\mathbf{u_e'}$ are assumed statistically independent from each other. Some studies, however, have proposed [101–103] schemes that include the (negative) cross-correlation between the alongwind and vertical components. In particular, Zannetti [104] updates the components u_x', u_y', and u_z' of $\mathbf{u_e'}$ according to

$$u_x'(t_2) = f_1 \, u_x'(t_1) + u_x''(t_2) \tag{61}$$

$$u_y'(t_2) = f_2 \, u_y'(t_1) + f_3 \, u_x'(t_2) + u_y''(t_2) \tag{62}$$

$$u_z'(t_2) = f_4 \, u_z'(t_1) + f_5 \, u_y'(t_2) + f_6 \, u_x'(t_2) + u_z''(t_2) \tag{63}$$

where u_x'', u_y'', u_z'' are uncorrelated zero-averaged Gaussian noises (i.e., random numbers) with standard deviations $\sigma_{u_x''}$, $\sigma_{u_y''}$, $\sigma_{u_z''}$, respectively. This system provides a recursive computation of u_x', u_y', and u_z' using the following meteorological input:

- Standard deviations $\sigma_{u_x'}$, $\sigma_{u_y'}$, and $\sigma_{u_z'}$ of the $\mathbf{u_e'}$ components
- Autocorrelations of the $\mathbf{u_e'}$ components with time lag Δt, i.e., $r_x(\Delta t)$, $r_y(\Delta t)$, $r_z(\Delta t)$
- Cross-correlations of the $\mathbf{u_e'}$ components with no time lag, i.e., $r_{xy}(0)$, $r_{xz}(0)$, $r_{yz}(0)$

Several studies have shown [105–107] that a vertical gradient in $\sigma_{u_z'}$ may cause an unrealistic accumulation of particles in regions of low $\sigma_{u_z'}$. Several semi-empirical formulations have been proposed to avoid this accumulation. According to these methods, if we neglect the cross-correlation terms, Equation 63 can be written as

$$u_z'(t_2) = \phi \, u_z'(t_1) + u_z''(t_2) + c \tag{64}$$

where

$$\phi = r_z(\Delta t) \tag{65}$$

$$\sigma_{u_z''} = \sigma_{u_z'} \, (1 - \phi^2)^{1/2} \tag{66}$$

$$c = a_d \, T \, [1 - \exp(-\Delta t/T)] \tag{67}$$

$$T = -\Delta t / \ln \phi \tag{68}$$

Two available formulas for the acceleration a_d can be used. The first is

$$a_d = \partial \sigma_{u_z'}^2 / \partial z \tag{69}$$

proposed by [107] and [108]; and the second is

$$a_d = \frac{1}{2}(\partial\sigma^2_{u_z'}/\partial z) \cdot (1 + [u_z'(t_1)/\sigma^2_{u_z'}]^2) \tag{70}$$

proposed by [105]. Both formulas use the vertical gradient of $\sigma^2_{u_z'}$ which is a meteorological input.

Advantages and Disadvantages of Particle Models

Dispersion simulation by Lagrangian particles has been called "natural" modeling. These models do not need the input of artificial stability classes, empirical sigma curves, or diffusion coefficients that are practically impossible to measure. Instead, diffusion characteristics are simulated by attributing a certain degree of "fluctuation" to each particle, using, for example, the computer's capability to generate semirandom numbers.

The basic advantages of this approach (e.g., [76, 77]) are:

- Compared with grid models, this method avoids the artificial initial diffusion of a point source in the corresponding cell and the advection numerical errors.
- This method is practically free of restricting physical assumptions, since all uncertainties are combined into the correct determination of pseudovelocities.
- Each particle can be tagged with its coordinates, source indicator, mass, activity, species, and size, allowing computation of wet and dry deposition, decay, and particle size distribution.
- If chemistry is required, a grid can be superimposed and concentrations in each cell computed by counting the particles of each species, allowing the use of any reaction scheme at each time step.*
- The meteorological input required can be inferred directly from measured data. The primary information needed is [77] the variance of wind velocity fluctuations and the Lagrangian autocorrelation function, which can be related to Eulerian measurements (e.g., Hanna, in [36]).

Potentially, the method is superior in both numerical accuracy and physical representativeness, as illustrated qualitatively in the examples of simulation in Figure 8. However, much research is still needed to extract, from meteorological measurements and our limited theoretical understanding of turbulence processes, the meteorological input required to run this model (i.e., the pseudovelocities to move each particle at each time step).

SPECIAL APPLICATIONS

The methodologies presented in the previous three sections can be applied to simulate atmospheric diffusion in simple (i.e., homogeneous, flat terrain) regions or in complex conditions, such as rough terrain, coastal diffusion, diffusion around buildings and heavy gas dispersion. A detailed treatment of these phenomena is clearly beyond the goals of this review; however, some general information and important references are presented below.

Rough Terrain

Dispersion in complex (rough) terrain is still poorly understood, even though recent dispersion experiments, such as the U.S. EPA Complex Terrain Model Development Project, have allowed important parameterization efforts of simplified cases (e.g., dispersion near an

* A rigorous concentration computation should not just add up the number of particles in a given cell at a given time. In fact, concentrations should be computed using the total time spent by each particle in the receptor volume during each time step (as in [78]).

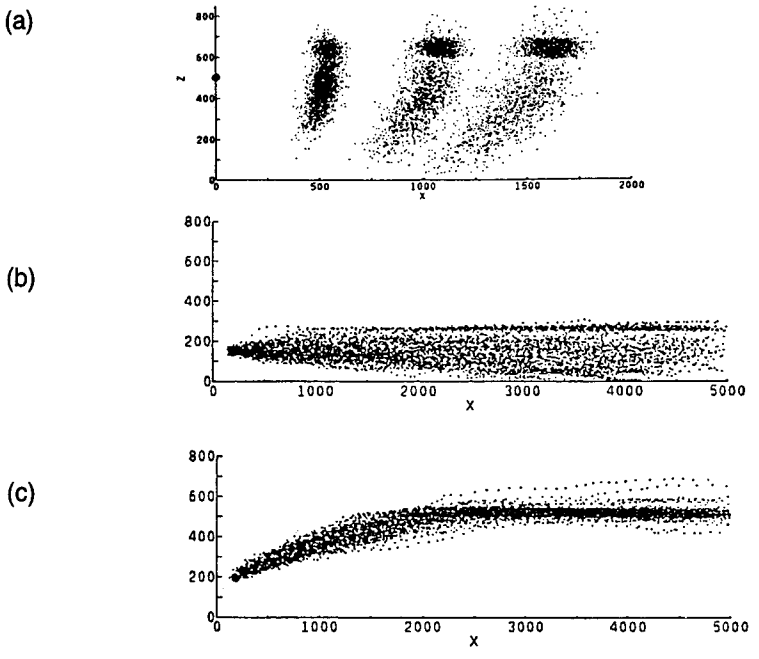

Figure 8. Qualitative behavior of a nonbuoyant puff (a), a nonbuoyant plume (b), and a buoyant plume (c), with an elevated inversion as simulated by particle models (from [78a]).

isolated small hill and plume impaction on it). The major problems in complex terrain applications are:

1. The correct evaluation of the trajectory of plume centerline and, in particular, its possible impaction upon the elevated terrain.
2. The computation of the enhancement of plume dispersion (in both the horizontal and the vertical) caused by the extra turbulence induced by the complexity of the terrain features.
3. The determination of possible effects caused by streamlines dividing around the terrain obstacles.

Egan [79] gives an overview of complex terrain modeling. Many studies [80–86] have focused on the "small hill" case. Snyder [87] has made a review of the case of pollutant transport and diffusion in stably, stratified flow. A report on air flow and dispersion in rough terrain has also been provided by Hunt et al. [88].

Coastal Diffusion

The literature contains reports of many studies in which air pollution dispersion near the shoreline of a large body of water is simulated with advanced numerical techniques in order to take into account the hydrodynamics of the breeze effect and the consequent dispersion [89–91]. Unfortunately, application of such methodologies requires extensive meteorological data input, which is generally not available, technical expertise in the selection of modeling parameters and the interpretation of results, and extensive computer time and storage. Therefore, for practical applications, these methods cannot currently be considered appro-

priate. However, they do provide realistic numerical simulations that should be considered in the development of simpler techniques.

A simple Gaussian model application in these circumstances has often given interesting results in spite of the complexity of the problem (e.g., [92]). Therefore, many studies have been developed for extending and improving the Gaussian formula to simulate coastal dispersion conditions. The work in [93] (further developed in [94]), postulates a stable Gaussian plume over the water surface advected over an unstable mainland surface, and gives a fumigation formula in which concentration is vertically homogeneous and varies only with the distance from the shoreline.

As discussed in [95], plume dispersion modules in coastal regions need to include the following calculations:

1. The thermal internal boundary layer (TIBL) height, i.e., the variation of the mixing height with the distance inland from the shoreline.
2. The dispersion rates inside the convective, unstable TIBL and the stable air above the TIBL.
3. The plume's partial penetration of the TIBL.
4. Overwater dispersion rates (if the plume is emitted offshore).

Diffusion Around Buildings

Several studies have tried to evaluate the dispersion behavior around buildings (see Figure 9) and a few of them have proposed empirical algorithms to simulate these peculiar effects. One of the commonest techniques is based on the studies of Huber and Snyder [96] and Huber [97] and has been incorporated into the U.S. EPA Industrial Source Complex model [98]. This technique is based on the results of tunnel experiments with a building crosswind dimension double that of the building height, and with atmospheric stability from C (slightly unstable) to D (neutral).

The first step in this wake-effect evaluation method [98] is to calculate the plume rise due to momentum alone. If the plume height, given by the sum of the stack height and the momentum rise at a downwind distance of two building heights, is greater than either 2.5 building heights ($2.5\ h_b$) or the sum of the building height and 1.5 times the building width ($h_b + 1.5\ h_w$), the plume is assumed to be unaffected by the building wake. Otherwise, the plume is assumed to be affected by the building wake.

Heavy Gas Dispersion

The production, transportation, and storage of large quantities of heavy gases represent a serious danger to the public. Heavy gas clouds constitute a severe environmental hazard. For example, a cloud of methane, propane, or butane [99] may be flammable if its mean volume concentration is higher than about 1%; a cloud of chlorine may be poisonous at concentrations of about 10^{-5}%!

Some modeling techniques have been proposed and tested for the simulation of heavy gas dispersion. Eidsvik [99] proposed a simple model in which the horizontal dimension of the cloud is assumed to increase due to the gravity fall of the cloud, and the cold cloud is heated from below and from air entrainment. The model predicts accurately some experimental data on heavy gas dispersion.

Zeman [100] investigated gravity currents and developed a simple one-layer model that simulates the formation of the gravity flow by boiling the spilled liquefied gas, the three-dimensional nature of the gravity flow in the presence of wind, and the convective heating and its contribution to the entrainment of ambient air. Zeman also identified the scaling laws of the above phenomena, which are shown to agree with the model predictions.

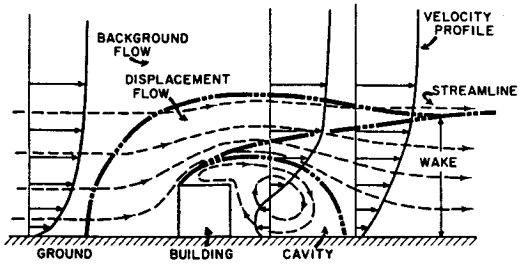

Figure 9. Mean flow around a cubical building. The presence of a bluff structure in otherwise open terrain will produce aberrations in the wind flow generally similar to those shown [60]. Reprinted with permission from the American Society of Mechanical Engineers.

Acknowledgments

Part of the material presented in this review article has been taken from the report* *Critical Survey of Mathematical Models of Atmospheric Pollution, Transport and Deposition,* prepared by Paolo Zannetti and Ivar Tombach for the Joint Research Center (JRC) of the Commission of the European Communities, Ispra Establishment. The author thanks Dr. Giuseppe Brusasca for reading the manuscript and useful suggestions.

We extend our appreciation to Ms. Barbara McMurray for her accurate typing of the manuscript, and to Ms. Anita Spiess for her editorial review.

REFERENCES

1. Panofsky, H. A., and J. A. Dutton, *Atmospheric Turbulence,* John Wiley & Sons, New York, 1984.
2. Pielke, R. A., *Mesoscale Meteorological Modeling,* Academic Press, Orlando, Fla, 1984.
3. Puttock, J. S., "Turbulent Diffusion from Sources Near Obstacles with Separated Wakes—Part II. Concentration Measurements near a Circular Cylinder in Uniform Flow," *Atmos. Environ. 13*:15–22 (1979).
4. Willis, G. E., and J. W. Deardorff, "A Laboratory Study of Dispersion from a Source in the Middle of the Convectively Mixed Layer," *Atmos. Environ. 15*:109–117 (1981).
5. Mitsumoto, S., and H. Ueda, "A Laboratory Experiment on the Dynamics of the Land and Sea Breeze," *J. Atmos. Sci. 40*:1228–1240 (1983).
6. Alessio, S., L. Briatore, G. Elisei, and A. Longhetto, "A Laboratory Model of Wake-Affected Stack Emissions," *Atmos. Environ. 17*:1139–1143 (1983).
7. Georgopoulos, P. G., and J. H. Seinfeld, "Statistical Distributions of Air Pollutant Concentrations," *Environ. Sci. Technol. 16*:401A–415A (1982).
8. Zannetti, P., "Short-Term Real-Time Control of Air Pollution Episodes in Venice," IBM Palo Alto Scientific Center Report No. G320-3371. Proceedings, 71st Annual APCA Meeting, Houston, TX, 1978.
9. Simpson, R. W., and A. P. Layton, "Forecasting Peak Ozone Levels," *Atmos. Environ. 17*:1649–1654 (1983).
10. Tiao, G. C., G. E. P. Box, and W. J. Hamming, "Analysis of Los Angeles Photochemical Smog Data: A Statistical Overview," *JAPCA 25*:260–268 (1975).

* AeroVironment Technical Report AV-FR-85/525, February 1986.

11. Cooper, J. A., and J. G. Watson, "Receptor Oriented Methods of Air Particulate Source Apportionment," *JAPCA 30*:1116–1125 (1980).
12. Kleinmann, M. T., S. Pasternack, M. Eisenbud, and T. J. Kneip, "Identifying and Estimating the Relative Importance of Sources of Airborne Particulates," *Envir. Sci. Technol. 14*:62–65 (1980).
13. Gordon, G. E., "Receptor Models," *Envir. Sci. Technol. 14*:792–800 (1980).
14. Watson, J. G., "Overview of Receptor Model Principles," *JAPCA 34*:619–623 (1984).
15. Henry, R. G., C. W. Lewis, P. K. Hopke, and H. J. Williamson, "Review of Receptor Model Fundamentals," *Atmos. Environ. 18*:1507–1515 (1984).

15a. Cooper, J. A., "Receptor Model Approach to Source Apportionment of Acid Rain Precursors," VIth World Congress on Air Quality, Paris, France, May 16–20, 223–229 (1983).

16. Dickerson, M. H., "MASCON—A Mass-Consistent Atmospheric Flux Model for Regions with Complex Terrain," *J. Appl. Meteorol. 17*:241–253 (1978).
17. Sherman, C. A., "A Mass-Consistent Model for Wind Fields Over Complex Terrain," *J. Appl. Meteor. 17*:312–319 (1978).
18. Patnack, P. C., B. E. Freeman, R. M. Traci, and G. T. Phillips, "Improved Simulations of Mesoscale Meteorology," Report Atmospheric Science Laboratory. White Sands Missile Range, N.Mex., ASL CR-83-0127-1, (1983).
19. Ludwig, F. L., and G. Byrd, "An Efficient Method for Deriving Mass-Consistent Flow Fields from Wind Observations in Rough Terrain," *Atmos. Environ. 14*:585–587 (1980).

19a. Danard, M., "A Simple Model for Mesoscale Effects of Topography on Surface Winds," *Mon. Weather Rev. 105*:572–581 (1977).

20. Bornstein, R., U. Pechinger, R. Miller, S. Klotz, R. Street, "Modeling the Polluted Coastal Urban Environment Vol. 1: The PBL Model," Final Report Prepared for Electric Power Research Institute, EA-5091, Volume 1; Research Project 1630-13, February, 1987.
21. Pielke, R. A., and Y. Mahrer, "Technique to Represent the Heated-Planetary Boundary Layer in Mesoscale Models with Coarse Vertical Resolution," *J. Atmos. Sci. 32*:2288–2308 (1983).
22. Briggs, G. A., "Plume Rise Predictions," *Lectures on Air Pollution and Environmental Impact Analyses* Workshop Proceedings, American Meteorological Society, Boston, Mass., 1975.
23. Golay, M. W., "Numerical Modeling of Buoyant Plumes in a Turbulent, Stratified Atmosphere," *Atmos. Environ. 16*:2373–2381 (1982).
24. Stern, A. C., Ed., *Air Pollution*, 3rd Edition, Volume I, Academic Press, New York, 1976.
25. Hanna, S. R., G. A. Briggs, and R. P. Hosker, Jr., "Handbook on Atmospheric Diffusion," Department of Energy Document DOE/TIC-11223 (DE82002045), 1982.
26. Briggs, G. A., "Plume Rise," AEC Crit. Rev. Ser., TID-25075. U.S. At. Energy Comm., Div. Tech. Inform. Ext., Oak Ridge, Ten (1969).
27. Turner, D. B., "Proposed Pragmatic Methods for Estimating Plume Rise and Plume Penetration Through Atmospheric Layers," *Atmos. Environ.*, Vol. 19, (7):1215–1218, 1985.
28. Bjorklund, J. D., and J. F. Bowers "User's Instructions for the SHORTZ and LONGZ Computer Programs, Vols. I and II, EPA-903/9-82-004A and B (NTIS Accession Numbers PB83-146 092 and PB83-146 100), U.S. Environmental Protection Agency, Middle Atlantic Region III.
29. Schatzmann, M., "An Integral Model of Plume Rise," *Atmos. Environ. 13*:721–731 (1979).

30. Stuhmiller, J., "Development and Validation of a Two-Variable Turbulence Model," Report SAI-74-509-LJ, Science Applications, Inc., La Jolla, CA (1974).
31. Glendening, J. W., J. A. Businger, and R. J. Farber, "Improving Plume Rise Prediction Accuracy for Stable Atmospheres with Complex Vertical Structure," *JAPCA 34*:1128–1133 (1984).
32. Anfossi, D., G. Bonino, F. Bossa, and R. Richiardone, "Plume Rise from Multiple Sources: A New Model," *Atmos. Environ. 12*:1821–1826 (1978).
33. Manins, P. C., "Partial Penetration of an Elevated Inversion Layer by Chimney Plumes," *Atmos. Environ. 13*:733–741 (1979).
34. Schatzmann, M., and A. J. Policastro, "An Advanced Integral Model for Cooling Tower Plume Dispersion," *Atmos. Environ. 18*:663–674 (1984).
35. Longhetto, A., Ed., *Atmospheric Planetary Boundary Layer Physics*, Elsevier Scientific Publishing Company, New York, 1980.
36. Nieuwstadt, F. T. M., and H. van Dop, Eds., *Atmospheric Turbulence and Air Pollution Modeling*, D. Reidel Publishing Company, Dordrecht, Holland, 1982.
37. Lewellen, W. S., and M. Teske, "Second-Order Closure Modeling of Diffusion in the Atmospheric Boundary Layer," *Boundary Layer Meteor. 10*:69–90, 1976.
38. Teske, M. E., and W. S. Lewellen, "Horizontal Roll Vortices in the Planetary Boundary Layer," Proceedings of the 4th Symposium on Turbulence, Diffusion, and Air Pollution, AMS, 456–463, 1979.
39. Lewellen, W. S., and R. I. Sykes, "Second-order Closure Model Exercise for the Kincaid Power Plant Plume," Electric Power Research Institute, report EA-3079 for Palo Alto, Calif., 1983.
40. Rounds, W., "Solutions of the Two-Dimensional Diffusion Equation," *Trans. Am. Geophys. Union 36*:395–405, 1955.
41. Demuth, C., "A Contribution to the Analytical Steady Solution of the Diffusion Equation for Line Sources," *Atmos. Environ. 12*:1255–1258, 1978.
42. Huang, C. H., "A Theory of Dispersion in Turbulent Shear Flow," *Atmos. Environ. 13*:453–463 (1979).
43. Tirabassi, T., M. Tagliazucca, and R. Lupini, "A Non-Gaussian Model for Evaluating Ground Level Concentration by Steady Sources," *Environmental Systems Analysis and Management*, S. Rinaldi, Ed., North-Holland Publ. Co., Amsterdam, 1982, pp. 627–635.
44. Tirabassi, T., M. Tagliazucca, and P. Zannetti "KAPPA-G, A NonGaussian Plume Dispersion Model: Description and Evaluation Against Tracer Measurements," *JAPCA 36*:592–596 (1986).
45. Richtmyer, R. D., and K. W. Morton, *Difference Methods for Initial-Value Problems*, Interscience Publishers, John Wiley and Sons, Inc., New York, 1967.
46. McRae, G. J., W. R. Goodin, and J. H. Seinfeld, "Mathematical Modeling of Photochemical Air Pollution," Environmental Quality Laboratory, Report No. 18, Pasadena, Calif. (1982). Also see: McRae, G. J., W. R. Goodin, and J. H. Seinfeld, "Development of a Second-Generation Mathematical Model for Urban Air Pollution—I. Model formulation," *Atmos. Environ. 16*(4):679–696 (1982).
47. Seinfeld, J. H., Atmospheric Chemistry and Physics of Air Pollution. John Wiley and Sons, New York, 1986.
48. U.S. Environmental Protection Agency, "Guideline on Air Quality Models," EPA-450/2-78-025, OAQPS No. 1.2-080, 1978.
48a. Williamson, S. J., *Fundamentals of Air Pollution*, Addison-Wesley Publishing Co., Reading, MA, 1973.
49. R. Pasquill, "Atmospheric Dispersion of Pollution," *J. Royal Meteor. Soc. 97*:369–395 (1971).

50. Taylor, G. I., "Diffusion by Continuous Movements," *Proc. London Math. Soc. Ser.*, 2(20):196 (1921).
51. Draxler, R. R., "Determination of Atmospheric Diffusion Parameters," *Atmos. Environ. 10*:99–105 (1976).
52. Pasquill, F., "Atmospheric Dispersion Parameters in Gaussian Plume Modeling—Part 2, Possible Requirements for Change in the Turner Workbook Values," EPA-600/4-76-030b, 1976.
53. Irwin, J. S., "Estimating Plume Dispersion—A Recommended Generalized Scheme," Presented at 4th AMS Symposium on Turbulence and Diffusion, Reno, Nev., 1979.
54. Hanna, S. R., et al., "AMS Workshop on Stability Classification Schemes and Sigma Curves—Summary of Recommendations," *Bull. Amer. Met. Soc. 58* (12):1305–1309 (1977).
55. Phillips, P., and H. A. Panofsky, "A Reexamination of Lateral Dispersion from Continuous Sources," *Atmos. Environ. 16*:1851–1859 (1982).
55a. Dobbins, R. A., *Atmospheric Motion and Air Pollution*, John Wiley & Sons, New York, 1979.
55b. DeMarrais, G. A., "Atmospheric Stability Class Determinations on a 481-Meter Tower in Oklahoma," *Atmos. Environ. 12*:1957–1964 (1978).
56. Gifford, F. A., "Use of Routine Meteorological Observations for Estimating the Atmospheric Dispersion," *Nuclear Safety* 2(4):47–57 (1961).
57. Turner, D. B., "Workbook of Atmospheric Dispersion Estimates," EPA, Research Triangle Park, AP-26 (NTIS PB 191-482) NC, 1970.
58. Green, A. E. S., R. P. Singhal, and R. Venkateswar, "Analytic Extensions of the Gaussian Plume Model," *JAPCA 30* (7):773–776 (1980).
59. Gifford, F. A., "Consequences of Effluent Release," *Nuclear Safety 17* (1):68–86 (1976).
60. Smith, M. E., *Recommended Guide for the Prediction of the Dispersion of Airborne Effluents* 1st edition, The American Society of Mechanical Engineers, New York, 1968.
61. Briggs, G. A., "Diffusion Estimation for Small Emissions, in Environmental Research Laboratories," Air Resources Atmospheric Turbulence and Diffusion Laboratory 1973 Annual Report ATDL-106, National Oceanic and Atmospheric Administration, 1974.
61a. Stern, A. C., R. W. Boubel, D. B. Turner, and D. L. Fox, *Fundamentals of Air Pollution*, Academic Press Inc., Orlando, FL, 1984.
62. McElroy, J. L., and F. Pooler, "St. Louis Dispersion Study—Vol. II, Analysis," National Air Pollution Control Administration Publication No. AP-53, U.S. Dept. of Health, Education and Welfare, Arlington, Va., 1968.
63. U.S. Environmental Protection Agency, "Guideline on Air Quality Models," EPA-450/2-78-027R, 1986.
64. Yamartino, R. J., Jr. "A New Method for Computing Pollutant Concentrations in the Presence of Limited Vertical Mixing," *APCA Note-Book 27*(5), 1977.
65. Hales, J. M., D. C. Powell, and T. D. Fox, "STRAM—An Air Pollution Model Incorporating Non-linear Chemistry, Variable Trajectories, and Plume Segment Diffusion," EPA 450/3-77-012 Research Triangle Park, N.C., 1977.
66. Benkley, C. W., and A. Bass, "Development of Mesoscale Air Quality Simulation Models—Vol. 3, User's Guide to MESOPUFF (Mesoscale Puff) model, EPA 600/7-79-XXX, Research Triangle Park, N.C., 1979.
67. Chan, M. W., S. J. Head, and S. Machiraju, "Development and Validation of an Air Pollution Model for Complex Terrain Application," Paper presented at NATO/CCMS Air Pollution Pilot Study, Rome, Italy. AeroVironment Technical Paper No. 9559, 1979.

68. Lamb, R. G., "An Air Pollution Model of Los Angeles," M.S. thesis, University of California, Los Angeles (see R. G. Lamb and M. Neiburger, "An Interim Version of a Generalized Urban Diffusion Model," *Atmos. Environ. 5*:239–264 (1969).
69. Roberts, J. J., E. S. Croke, and A. S. Kennedy, "An Urban Atmospheric Dispersion Model," Symposium on Multiple-Source Urban Diffusion Models, Air Pollution Control Office Publ. No. AP-86, 1970.
70. Sheih, C. M., "A Puff Pollutant Dispersion Model with Wind Shear and Dynamic Plume Rise," *Atmos. Environ. 12*:1933–1938 (1978).
71. Ludwig, F. L., L. S. Gasiorek, and R. E. Ruff, "Simplification of a Gaussian Puff Model for Real-Time Minicomputer Use," *Atmos. Environ. 11*:431–436 (1977).
72. Zannetti, P., "An Improved Puff Algorithm for Plume Dispersion Simulation," *J. Applied Met. 20* (10):1203–1211 (1981)
73. Zannetti, P., "A New Mixed Segment-Puff Approach for Dispersion Modeling," *Atmos. Environ. 20*(6):1121–1130 (1986).
74. Seinfeld, J. H., *Air Pollution—Physical and Chemical Fundamentals*, McGraw-Hill, New York, 1975.
75. Hockney, R. W., and J. W. Eastwood, *Computer Simulation Using Particles*, McGraw-Hill, New York, 1981.
76. Lange, R., "ADPIC—A Three-Dimensional Particle-in-Cell Model for the Dispersal of Atmospheric Pollutants and Its Comparison to Regional Tracer Studies," *J. Appl. Meteor. 17*:320 (1978).
77. Lamb, R. G., H. Hogo, and L. E. Reid, "A Lagrangian Monte Carlo Model of Air Pollutant Transport, Diffusion and Removal Processes," 4th AMS Symposium on Turbulence, Diffusion and Air Pollution, Reno, Nev, 1979.
78. Lamb, R. G., H. Hogo, and L. E. Reid, "A Lagrangian Approach to Modeling Air Pollutant Dispersion-Development and Testing in the Vicinity of a Roadway," EPA-600/4-79-023, 1979.
78a. Zannetti, P., and N. Al-Madani "Simulation of Transformation, Buoyancy, and Removal Processes by Lagrangian Particle Methods," Fourteenth ITM Meeting on Air Pollution Modeling and Its Application. Copenhagen, Denmark, September 1983.
79. Egan, B. A., Sc. D., "Transport and Diffusion in Complex Terrain," *Boundary-Layer Met. 30* (1984).
80. Sacre, C., "An Experimental Study of the Airflow over a Hill in the Atmospheric Boundary Layer," *Boundary Layer Meteor. 17*:381–401 (1979).
81. Mason, P. J., and R. I. Sykes, "Flow Over an Isolated Hill of Moderate Slope," *J. Royal Meteor. Soc. 105*:383–395 (1979).
82. Hunt, J. C. R., J. S. Puttock, and W. H. Snyder, "Turbulent Diffusion from a Point Source in Stratified and Neutral Flows around a Three-Dimensional Hill—Part I, Diffusion Equation Analysis," *Atmos. Environ. 13*:1227–1239 (1979).
83. Britter, R. E., J. C. R. Hunt, and K.J. Richards, "Air Flow Over a Two-Dimensional Hill: Studies of Velocity Speed-up, Roughness Effects and Turbulence," *J. Royal Soc. 107*:91–110 (1981).
84. Taylor, P. A., and J. L. Walmsley, "Estimates of Wind-Speed Perturbation in Boundary-Layer Flow Over Isolated Low Hills—A Challenge," *Boundary Layer Meteor. 20*:253–257 (1980).
85. Jenkins, G. J., P. J. Mason, W. H. Moores, and R. I. Sykes, "Measurements of the Flow Structure Around Ailsa Craig, a Steep, Three-Dimensional, Isolated Hill," *J. Royal Met. Soc. 107*:833–851 (1981).
86. Ryan, W., and B. Lamb, "Determination of Dividing Streamline Heights and Froude Numbers for Predicting Plume Transport in Complex Terrain," *JAPCA 31*:152–155 (1984).
87. Snyder, W. H., "Fluid Modeling of Pollutant Transport and Diffusion in Stably Stratified Flows over Complex Terrain," *Ann. Rev. Fluid Mech. 17*:239–66 (1985).

88. Hunt, J. C. R., D. P. Lalas, and D. N. Asimakopoulos, "Air Flow and Dispersion in Rough Terrain: A Report on Euromech 173," *J. Fluid Mech. 142*:201–216 (1984).
89. Bornstein, R. D., and E. Runca, "Preliminary Investigations of SO_2 Patterns in Venice, Italy Using Linked PBL and K-Models, Including Removal Processes," Proceedings of the AMS Joint Conference on Applications of Air Pollution Meteorology, Salt Lake City, Utah, 1977.
90. Dieterle, D. A., and A. G. Tingle, "A Numerical Study of Mesoscale Transport of Air Pollutants in Sea-Breeze Circulations," Proceedings of the 4th AMS Symposium on Turbulence, Diffusion and Air Pollution, Reno, Nev., 1977.
91. Dobosy, R., "Dispersion of Atmospheric Pollutants in Flow Over the Shoreline of a Large Body of Water," *Appl. Meteor. 18*:117–132 (1977).
92. Runca, E., P. Melli, and P. Zannetti, "Computation of Long-term Average SO_2 Concentration in the Venetian Area," *Appl. Math. Model. 1*:9–15 (1976).
93. Lyons, W. A., and H. S. Cole, "Fumigation and Plume Trapping on the Shores of Lake Michigan during Stable Onshore Flow," *J. Appl. Meteor. 12*:494–510 (1973).
94. van Dop, H., R. Steenkist, and F. T. M. Nieuwstadt, "Revised Estimates for Continuous Shoreline Fumigation," *J. Appl. Meteor. 18*:133–137 (1979).
95. Stunder, M., and S. SethuRaman "A Statistical Evaluation and Comparison of Coastal Point Source Dispersion Models," *Atmos. Environ. 20*(2):301–315 (1986).
96. Huber, A. H., and W. H. Snyder, "Building Wake Effects on Short Stack Effluents," Preprint volume for the 3rd AMS Symposium on Atmospheric Diffusion and Air Quality, Boston, Mass. (1976).
97. Huber, A. H., "Incorporating Building/Terrain Wake Effects on Stack Effluents," Preprint volume for the AMS Joint Conference on Applications of Air Pollution Meteorology, AMS, Boston, Mass., 1977.
98. Bowers, J., J. Bjorklund, and C. Cheney, "Industrial Source Complex (ISC) Dispersion Model User's Guide, Vol. I," EPA-450/4-79-030, Research Triangle Park, N.C., (1979).
99. Eidsvik, K. J., "A Model for Heavy Gas Dispersion in the Atmosphere," *Atmos. Environ. 14*:769–777 (1980).
100. Zeman, O., "The Dynamics and Modeling of Heavier-Than-Air, Cold Gas Releases," *Atmos. Environ. 16*:741–751 (1982).
101. Zannetti, P., "An Improved Puff Algorithm for Plume Dispersion Simulation," *J. Applied Met., 20*(10): 1203–1211, (1981).
102. Ley, A. J., "A Random Walk Simulation of Two-Dimensional Turbulent Diffusion in the Neutral Surface Layer," *Boundary Layer Meteor., 10*: 69–90, (1982).
103. Legg, B. J., "Turbulent Dispersion from an Elevated Line Source: Markov Chain Simulations of Concentration and Flux Profiles," *Quart. J. R. Met. Soc., 109*: 645–660, (1983).
104. Zannetti, P., "Monte-Carlo Simulation of Auto- and Cross-correlated Turbulent Velocity Fluctuations (MC-LAGPAR II Model)," *Environ. Software, 1*(1): 26–30, (1986).
105. Wilson, J. D., G. W. Thurtell, and G. E. Kidd, "Numerical Simulation of Particle Trajectories in Inhomogeneous Turbulence, III: Comparison of Predictions with Experimental Data for the Atmospheric Surface Layer," *Boundary Layer Meteor., 12*: 423–441, (1981).
106. McNider, R. T., "Investigation of the Impact of Topographic Circulations on the Transport and Dispersion of Air Pollutants," Ph.D. dissertation, University of Virginia, page 210, (1981).
107. Legg, B. J. and M. R. Raupach, "Markov-Chain Simulation of Particle Dispersion in Inhomogeneous Flows: The Mean Drift Velocity Induced by a Gradient in Eulerian Velocity Variance," *Boundary Layer Meteor., 24*: 3–13, (1982).
108. Ley, A. J. and D. J. Thomson, "A Random Walk Model of Dispersion in the Diabatic Surface Layer," *Quart. J. Roy. Met. Soc., 109*: 847–880, (1983).